Piloted Simulation of Helicopter Shipboard Recovery with Visual and Control Augmentation

Tim Mehling[1], Omkar Halbe[2], and Manfred Hajek[3]
Technical University of Munich, 85748 Garching, Germany

Milan Vrdoljak[4]
University of Zagreb, 10002 Zagreb, Croatia

Shipboard launch and recovery of helicopters continue to pose operational challenges even for experienced pilots. The factors affecting pilot workload include unsteady ship motion, the influence of ship air wakes on helicopters, insufficient visual cues, and adverse weather conditions. The goal of the current research is to investigate novel visual and control augmentation techniques and evaluate their impact on pilot workload and handling qualities for shipboard recovery operations. This paper first outlines a helicopter-ship dynamic interface model developed and integrated into our existing rotorcraft simulation environment (ROSIE). It then describes a visual augmentation concept using a see-through helmet-mounted display (HMD) system for enhancing the pilot's visual cueing environment during the shipboard approach and landing tasks. Next, it describes the synthesis of robust nonlinear control laws for achieving advanced helicopter response types with predicted Level 1 handling qualities. Lastly, the paper reports the results of simulation tests of maritime mission task elements by four experimental test pilots with different levels of augmentation and under different environmental conditions. Results on navigation performance, workload indices, and handling quality ratings indicate a decreased workload and improved handling qualities to almost Level 1 with the assistance of the visual and control augmentation system. Moreover, all piltos stated a higher situational awareness while operating in degraded visual environment conditions using visual and control augmentation.

Acronyms

ACAH	=	Attitude Command/ Attitude Hold
ACVH	=	Acceleration Command/ Velocity Hold
AFCS	=	Automatic Flight Control System
DDG	=	Destroyer Designated Guided
DIPES	=	Deck Interface Pilot Scale
DVE	=	Degraded Visual Environment
ESLS	=	Enhanced Ship Deck Landing Symbology
HMD	=	Helmet-Mounted Display

[1] PhD candidate, Institute of Helicopter Technology, Departmentof Aerospace and Geodesy, Boltzmannstraße 15, AIAA student member
[2] PhD candidate, Institute of Helicopter Technology, Departmentof Aerospace and Geodesy, Boltzmannstraße 15, AIAA student member
[3] Professor, Institute of Helicopter Technology, Departmentof Aerospace and Geodesy, Boltzmannstraße 15, Senior AIAA member
[4] Professor, Faculty of Mechanical Engineering and Naval Architecture, Senior AIAA member

HQ	=	Handling Qualities
HSDI	=	Helicopter Ship Dynamic Interface
LAMP	=	Large Amplitude Motions Program
MTE	=	Mission Task Element
PAS	=	Pilot Assistance System
PID	=	Pilot Identification Number
PH	=	Position Hold
ROSIE	=	Rotorcraft Simulation Environment
SCONE	=	Systematic Characterization of the Naval Environment
SD	=	Standard Deviation
SLS	=	Ship Deck Landing Symbology
TLX	=	Task Load Index
TRC	=	Translational Rate Command

I. Introduction

Shipboard recovery of helicopters is one of the most challenging tasks for even the most experienced of pilots. The maritime environment including the helicopter and the ship, also known as the helicopter ship dynamic interface (HSDI), is highly uncertain. Sea swell, particularly in high sea states, causes rapid temporal and spatial variations to the ship motion about its degrees of freedom in the pitch, roll, and heave axes. The airwakes from the ship structure also influence the helicopter's dynamic motion. To land in such uncertain conditions, helicopter pilots require external visual cues for guidance. However, the HSDI is known to be rather poor at offering visual cues that the pilot can reliably use for the landing task [1]. Poor weather and night conditions further exacerbate visibility by obscuring the ship structure and the horizon reference. Furthermore, many conventional helicopters are known to have highly coupled and often unstable dynamics in hover and low-speed, which adds to the piloting difficulty [2]. Previous studies [3] [4] have shown that a combination of all these factors contributes to a significantly high pilot workload during the shipboard landing phases.

Technological aids have long been considered key to alleviating pilot workload, improving safety, and expanding a helicopter's maritime operational envelope [1]. Notably, technologies that enrich the visual cueing environment would naturally enhance the pilot's awareness of the helicopter's motion, position, and orientation relative to the landing spot. Among the promising ones are helmet-mounted and head-mounted display (HMD) systems, which allow the pilot to remain 'eyes-out' while retaining focus on important aircraft parameters. Reference objects in the far field can be readily supplemented by their three-dimensional (3-D) virtual copies in the near field via appropriate conformal symbology. By virtue of the visual cueing system being fixed to the pilot's head, the need for additional eye or head movement during physically and mentally demanding tasks is obviated [5]. Complementary to visual augmentation is control augmentation in the form of advanced flight control laws. Flight control systems hosting advanced control laws enhance the helicopter's flying qualities and allow the pilot to maneuver aggressively and with greater precision. Control laws can be readily configured to offer different levels of augmentation so that pilots always experience a precise, predictable, and stable aircraft dynamic behavior over the flight envelope of interest [6].

The real benefit of such technological aids can only be ascertained through extensive testing and evaluations. Doing so at substantially lower costs, however, requires a representative simulation environment of the helicopter ship dynamic interface. Such a simulation environment is typically composed of different modeling elements: an accurate helicopter flight dynamics model, a realistic ship motion, and aerodynamic interactions between the ship structure and the helicopter [7]. These modeling elements are hosted in suitable visual and motion cueing environments that include a cockpit setup and a visualization of the ship motion and the sea surface. In the context of piloted simulation testing, the fidelity of the chosen simulation environment assumes significance. Wilkinson et al. [8] suggest that the required level of fidelity is task-dependent: a high fidelity simulation environment is necessary for accurate flight flight envelope prediction, as an alternative to, or in support of at-sea trials; whereas a low fidelity simulation may suffice for eyes-out evaluations. Furthermore, the need for motion cueing versus having a fixed-base cockpit has been subject to much debate. Based on piloted simulation testing, Wang et al. [4] conclude that motion cueing has no perceivable effect in good visual conditions, but may cause differences in the pilot's workload ratings in poor visual conditions. Thus, a low- to medium-fidelity, fixed-base HSDI simulation setup can still offer an economical means for repeatable testing, tuning, and evaluation of pilot assistance features, before then proceeding to at-sea qualification trials. Not only does this setup facilitate qualitative and quantitative evaluation of the systems, but it can also offer critical insights into their impact on human factors in the helicopter ship dynamic interface.

The goal of the current research is to investigate novel visual and control augmentation techniques and evaluate their impact on pilot workload and handling qualities for the shipboard recovery task. The paper outlines the development and integration of a new helicopter ship dynamic interface model into our wide field-of-view, fixed-base cockpit rotorcraft simulation environment (ROSIE) [9]. For visualization purposes, the ship structure was modeled as a generic surface combatant of the DDG-51 class [10]; whereas the ship's motion was simulated using the Systematic Characterization of the Naval Environment (SCONE) empirical data [11]. The SCONE data offer three levels of deck motion intensity in the heave and roll axes. The paper further describes the design of a novel pilot assistance system (PAS) for visual and control augmentation. The PAS consists of a see-through helmet-mounted display (HMD) [12] for the visualization of a novel shipboard landing symbology (SLS). The HMD system was designed to enrich the pilot's visual cues by combining head-fixed aircraft parameter display with 3-D conformal shipboard landing cues. The PAS also includes four advanced control response-types, namely translational rate command with position hold (TRC/PH), acceleration command with velocity hold (ACVH), yaw rate command with direction hold (RCHH), and vertical rate command with height hold (RCHH), which were developed and tuned to comply with current helicopter handling qualities criteria (ADS-33E-PRF, [13]). These response-types essentially transform a demanding pilot task viz. stabilization and control to merely a task of precise steering/guiding the aircraft at the desired speed, altitude, and direction. It was hypothesized that improved visual cues would significantly improve the pilot's situational awareness, and that easing the guidance task would substantially enhance helicopter handling. The combined effect of these systems would alleviate pilot workload during the shipboard landing phases. These hypotheses were confirmed by simulation testing conducted with four maritime experimental pilots for different intensities of ship motion and different modes of the pilot assistance system.

The remainder of the paper is structured as follows. Section II reviews prior work on rotorcraft simulation testing in the maritime environment. Section III outlines the development of a helicopter ship dynamic interface environment. Section IV describes the design of a novel pilot assistance system including visual and control augmentation. Section V describes the experimental setup for the HSDI piloted simulation testing. Section VI presents the simulation results and discusses the human factors impact of the proposed pilot assistance system. Finally, Section VII collects the main conclusions.

II. Literature Review

Landing in adverse weather conditions is a typical mission in day-to-day helicopter operations [14]. When outside visual cues disappear, the overall workload on the pilot and the loss of SA increases [15]. Wartmann et al. characterize in the final report of HELI-X [16] outside visual cues disappear caused by situations whereas the helicopters main rotor downwash raises surrounding particles like dust (brownout), snow (whiteout), or even water during an offshore approach towards a ship. Upcoming situations, named as Degraded Visual Environments (DVEs) may lead to incidents like obstacle or ground hits. Padfield et al. [17] identify and transfer similar situations arising during dynamic [18] helicopter offshore operations in coordination with ships [19]. Operating maritime helicopters to naval ships at open sea is often a difficult and dangerous task. A restricted landing area which is pitching, rolling, and heaving, the pilot also deals within a harsh maritime environment where bad weather conditions often come across. The task of approaching and landing the helicopter in bad weather situations is acknowledged as being both demanding and dangerous [20]. Moreover, the pilot must contend with a highly dynamic restricted landing area [21]. For typical procedures [22], even during Instrument Meteorological Conditions (IMC) conditions, mission safety is enhanced by offering the pilots assistance systems on helicopter and ship side. Challenges within the shipborne environment [23] arise from ship airwake/ turbulence, ship motion, confined landing area, and visual cue limitations.

Piloted simulation using advanced response types such as ACVH and TRC/PH during helicopter ship operations indicated best performance while workload decreased. Almost Level 1 handling qualities and minimized pilot workload were achieved as supported by time domain metrics [24] [25]. However, flight tests identified DVEs on pilot workload as first limits for safe operation [26]: DVE and turbulence increased workload and reduced piloting performance, and had an impact on control input activity. On top, fullfilling specific rotorcraft tasks, such as hover behind, alongside and over the deck, and land, the motion cueing effect turned out to be more significant during DVE than ship air wakes [27]. In Ref. [27], a motion cueing simulation study of lateral sidestep manoeuvre indicated the importance of motion cueing. It was reported that without motion cues the pilot could not achieve the desired accuracy without heavily over-controlling. It was found that under the test points, although motion cueing could cause differences in the pilot's workload ratings, it had no discernible regular trend in the relative GVE. However, in the severely DVEs, the motion cueing effect was more significant. The pilot's workload ratings and control activities on control sticks and pedal were normally higher without motion cues. Consistent with previous studies [4] [28], our findings suggest that external visual cueing is vital for a successful landing, in particular during the last phases of landing. Therefore, based on the pilots' statements, we provide suggestions for possible improvements of external visual cues that have the potential to reduce pilots' workload and improve the overall safety of landing operations. During operational flight tests, pilots workload ratings and control activites were normally higher without any motion cues [27]. Therefor, one of the main benefits of a visual augmentation [28] is to reduce pilots' workload and increase SA in all phases of flight. Münsterer et al. [29] analyses together with helicopter pilots have shown that the preferred HMD display information depends on the phase of flight, the current environmental conditions and the visibility of the moving landing zone, the ship deck. Zimmermann et al. [30] investigated in HMD visual augmentation of a detected landing zone in flight using the ACT/FHS of the Deutsches Zentrum für Luft- und Raumfahrt e.V. (DLR): The resulting SferiAssist® [31] combines sucessfully tunnel in the sky symbology with dynamic path visualization based on a LIDAR sensor. Challenges arise when succesful onshore systems are transered to offshore operations, as done within this work. Investigations have been proceeded to differentiate impacts of pilot workload caused by visual cueing [32]. Results showed high differences in gaze patterns fullfilling approach and landing maneuvers onshore and offshore. However, no significant differences were observed between pilot control techniques in both environments for a given aircraft response type. Finally, simulated flight trials were proceeded, where test pilots conducted deck landings within an operational environment including ship motions, air wakes and different weather sceneries [33]. Landing a helicopter on a ship deck during DVE conditions is stated as a challenging endeavour, especially when avialable visual cues are limited.

III. Simulation of Helicopter Ship Dynamic Interface

The simulation environment in this work consists of a wide-screen, high-fidelity rotorcraft simulation environment (ROSIE), as shown in Figure 1. The key components of ROSIE [34] are a comprehensive, nonlinear dynamics model of a full-scale helicopter, an image generator with a six-channel dome projection system for the external visual cueing environment, and a fixed-base BO-105 cockpit including the essential human-machine interfaces.

The helicopter dynamics model in ROSIE uses the software package Generic Simulation (GenSim), which is a real-time-capable, comprehensive rotorcraft code for global steady and unsteady performance, flight mechanics, loads calculations, and flight simulations. GenSim assumes the main and tail rotor blades to be rigid. It simulates up to the first harmonics of the flap, lead-lag, and torsion modes using the blade element theory and simple analytical downwash models. The forces and moments are computed from the cumulative influence of the individual structural components – main rotor, tail rotor, fuselage, and empennage – using nonlinear aerodynamic coefficients and wind tunnel data. GenSim further includes models of the engine, rotor speed, and one DOF landing skid model. The structural and aerodynamic parameters supplied to GenSim are representative of the BO-105 helicopter, which is a light, multipurpose, twin-engine helicopter with a hingeless main rotor and a tail rotor. For the interested reader, Refs. [35] and [36] describe GenSim's internal code structure in greater detail, and Ref. [37] compares similar state-of-the-art comprehensive rotorcraft models.

Figure 1: Rotorcraft Simulation Environment

For the external visual cueing environment, a six-channel projection system provides a 200° horizontal field-of-view and -50°/+30° vertical field-of-view, as shown in Figure 1. Each projector has a resolution of 1920 pixels x 1200 pixels, which provides a resolution of about three minutes of arc per pixel depending on the field-of-view of each projector. An auto-calibration system allows the fusion of each channel into one homogenous picture projected onto the dome surface, yielding excellent warping and blending across the dome and at each channel intersection.

The BO-105 cockpit setup, as given in Figure 2, includes its original pilot inceptors: a centre stick, a collective lever, foot pedals, and a seat shaker for motion cueing. The center stick has a built-in force trim system that allows the pilot to change the detent position using a beep switch. The collective stick and pedals, however, do not include force trims. Despite having a fixed-based cockpit setup, the loads and vibrations experienced in a true cockpit are simulated by a seat shaker device installed underneath the pilot's seat. The seat shaker produces vibrations within a frequency range of 5 Hz to 200 Hz corresponding to the rotor harmonics and an amplitude as a function of the instantaneous normal load factor. Likewise, a synthetic acoustic environment in the cockpit is produced by stereo speakers. The audio setup modulates a pre-recorded, in-flight audio signal by the instantaneous rotor frequency, the speeds of the twin engines, and the normal load factor.

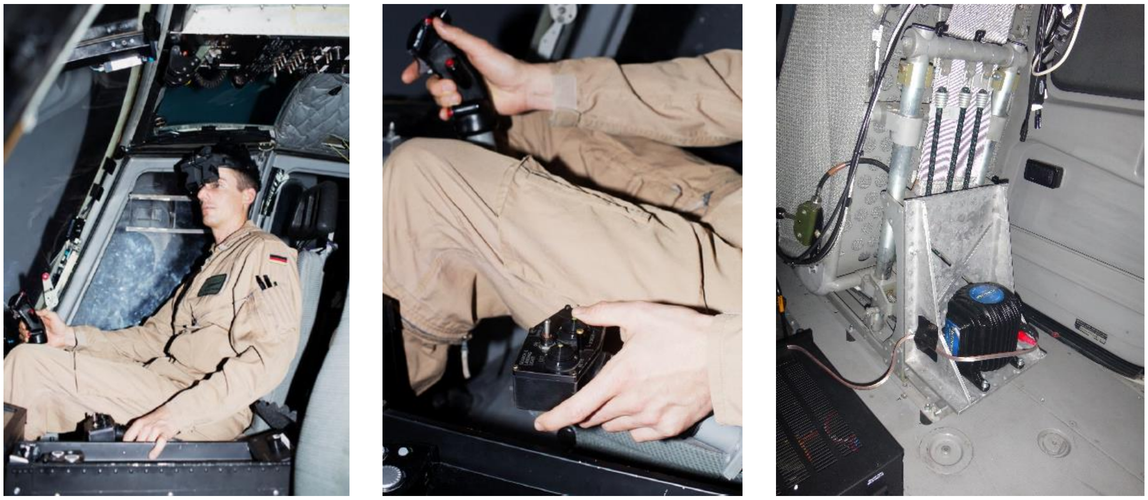

Figure 2: Cockpit configuration

Touch-screen displays that replace the original instrument panel of the BO-105 provide a complete display of the primary flight information, as given in Figure 3. A standard state-of-the-art head-down display (HDD) [39] approach was used during all flights subdivided into a PFD, and a digital moving map visualized on a separate MFD below the PFD. While PFD visualized H135 PFD information, digital moving map showed helicopters position on a typical aeronautical map (Scale 1:100.000).

Figure 3: HDD display configuration

An exhaustive description of ROSIE is omitted here for brevity; instead, the interested reader is referred to Ref. [41] for its complete hardware and softare architecture. The mentioned setup was previously used for onshore piloted simulation testing of visual augmentation methods in degraded visual environments [38]. In those tests, subjective ratings revealed an overall acceptable simulation fidelity with regards to the visual cueing system, the flight dynamics model, and the primary flight control system.

Building upon this basic ROSIE setup, the current research sought to develop a new, realistic simulation environment of the helicopter/ship dynamic interface. The first step in this direction was to integrate a structural model of the ship into the external visual cueing environment. Figure 5 shows the model of a DDG-51 destroyer class as seen on the ROSIE dome projection, along with a public aerial image of a real ship for comparison. The helicopter landing spot is located 130 m longitudinally aft of the ship's forward perpendicular on the ship lateral centerline and 5 m above the waterline.

In the next step, the dynamic ship motion was simulated using empirical data. The U.S. Office of Naval Research gathered these data under the Systematic Characterization of the Naval Environment (SCONE) program [43] and kindly made them available to the authors for scientific research purposes. Previous works that demonstrated autonomous recovery of helicopter from ships have also used the SCONE data [44] [45] [46]. The SCONE data consist of diverse sets of recordings that characterize the deck motion intensity in terms of the maximum amplitudes of the ship's roll and heave motion. **Fehler! Verweisquelle konnte nicht gefunden werden.** plots the time-domain roll and heave motion data taken from SCONE for the three levels of intensity. The SCONE data classifies deck motion intensity into low, medium, and high. An overview of the SCONE data characteristics is given in Table 1. Each level of intensity includes five different recordings, each with a sampling rate of 20 Hz.

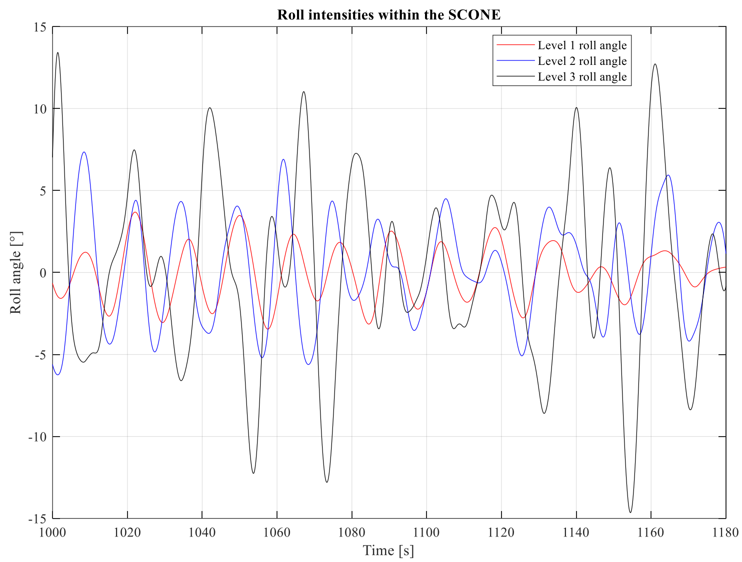

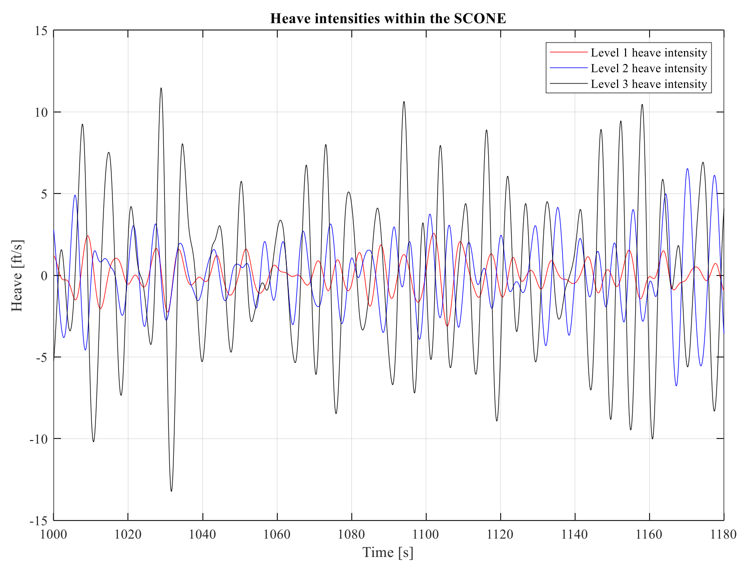

Figure 4. Roll (top) and heave (bottom) intensity levels within the SCONE database

Table 1. SCONE scaling within ROSIE

WMO Waves Description [48]	Wave Characteristics (m)	Ocean Waves Scale in ROSIE	SCONE levels within ROSIE
Slight	0.0 to 0.5	Low	1
Moderte	0.5m to 4.0	Moderate	2
High	4.0 to 6.0	High	3

The database is provided for the simulated deck motions using a state-of-the-art, nonlinear seakeeping prediction code (LAMP) [48] for animating the simulated ship via SCONE data. The dataset includes a full, consistent set of six degrees of freedom ship deck motion data for a generic surface combatant ship, DTMB Model 5415 hull, which is a representative of a DDG-51-type destroyer as shown in Figure 5.

Figure 5. (Left) Ship 3-D structural model, ship motion model, and sea swell model in ROSIE; (Right) Aerial image of DDG-51 class destroyer [40]

The LAMP predictions are time-domain simulations that incorporate a nonlinear calculation of the incident wave forcing and hydrostatic restoring, a body-linear 3-D potential flow solution of the wave-body hydrodynamic interaction forces (radiation, diffraction, and forward speed) and semi-empirical models for viscous roll damping and drag, appendage (rudder and bilge keel) lift and drag, propeller thrust and hull maneuvering forces. The propeller of the ship is operated at a constant rotation rate corresponding to a command calm water speed, so that the basic simulations include an unsteady variation in speed, although this variation is small for the selected conditions.

The next step was to achieve a high-fidelity simulation of the ocean surface, which is an important element to recreate a realistic HSDI visual environment [49]. For this purpose, a frequency-domain approach was adopted, which was introduced by Mastin et al. in Ref. [47]. This approach uses the Fast Fourier Transform (FFT) to transform random, temporally modified spectra into a height field representing the ocean. Although this method produces calm ocean surfaces, it was later improved by Tessendorf in Refs. [50] [51] to not only compute the height field but also simulate the wave displacements in the horizontal plane. Using frequencies and range parameters, this improved approach leads to the desired rendering of choppy waves, as seen in Figure 2. Finally, to render whitecaps at either the peak or at the intersections of the waves, the theory of Dupuy and Bruneton in Ref. [52] and Tessendorf in Ref. [50] was integrated into the wave model.

Finally, it is noted that aerodynamic interactions between the ship structure airwakes and the helicopter dynamics were not part of the simulation environment, since this is currently work in progress [53]. Although ship-helicopter aerodynamic interactions form an important element in the HSDI in general and particularly so for the prediction of operational limits and flight envelopes [54], the present research sought to focus on the human factors impact of technological aids during what was essentially an 'eyes-out-of-the-window' task [8] [55].

IV. Pilot Assistance System Development

The cognitive challenges associated with the helicopter ship dynamic interface have been well documented [1] [43] [56]. The cues and references associated with the ship and the external environment can often be limited, obscured, or uncertain. Aside from acquiring and processing external cues, pilots need to monitor critical aircraft parameters and maintain the helicopter within its safe flight envelope. These tasks force pilots to monitor data from disparate and spatially distributed sources concurrently, and in particular during the shipboard landing phase. Given the physical and cognitive limits of even the most experienced pilots, long mission durations and single-pilot operations can easily result in a high workload, fatigue, and reduced attention. A failure to maintain the required level of situational awareness can result in fatalities.

Thus, shipboard recovery missions demand assistance systems that can supply coherent and consistent information on a single, head-fixed display format without imposing additional constraints on the pilot. A judicious combination of intuitive visual and control augmentation techniques, thus, becomes the natural route to not only improve pilot situational awareness but also guarantee good handling qualities [1]. The development of two such novel visual and control augmentation systems is discussed next.

A. Visual Augmentation Using Helmet-Mounted Display

The simulation tests in this research used a HMD system as the basis for augmenting the pilot's visual cueing environment in the shipboard landing task. The ROSIE HMD system, called LCD-29 and developed by Trivisio, is low-cost and available for off-the-shelf purchase [57]. The LCD-29, shown in Figure 6 left, is a binocular HMD system with modified combiners (30% reflection, 70% transmission) for see-through capability in the simulation environment with reduced brightness compared to the real world. It consists of two full-color liquid crystal displays (LCD), each with a resolution of 800x600 pixels and a field-of-view of 23° horizontally and 17° vertically. Two separate input interfaces enable the generation of two different images for a stereoscopic presentation and a dynamic vergence adjustment. Reference [57] provides the complete technical specification of the LCD-29.

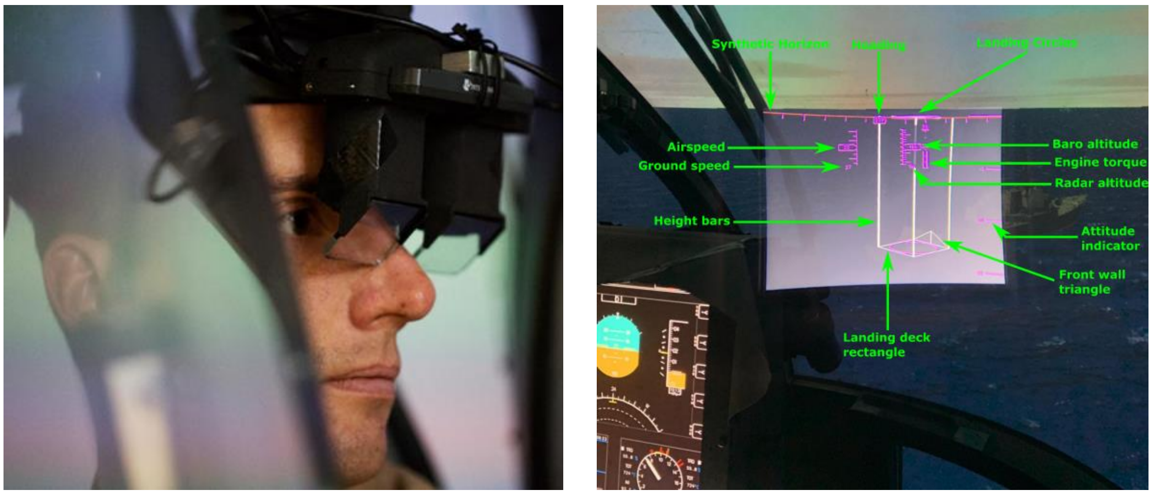

Figure 6. The HMD system (left) and the SLS concept (right)

Towards an intuitive landing assistance display concept, the present research led to the development of a new three-dimensional (3-D) dynamic shipboard landing symbology (SLS) concept and its integration into the LCD-29 HMD system. Figure 6 shows the SLS concept superimposed on the ship, as seen from the HMD system lens from the pilot's normal seating position. This SLS concept extends previous experimental works on visual cueing enhancements for DVE conditions [58] [59] and adapts the symbol concepts developed therein for the present shipboard landing task. In addition to the two-dimensional (2-D) primary flight information display, SLS provides 3-D visual cues to assist the pilot during the shipboard landing task.

The 2-D information display consists of head-fixed primary flight data and a helicopter-fixed attitude indicator. With reference to Figure 6, the primary flight data consists of airspeed, ground speed, heading, barometric altitude, radar altitude, and engine torque. The SLS 3-D concept shown in Figure 6 comprises the following elements:

1. Two landing circles connected via four height bars to show the altitude and position of the approaching helicopter relative to the landing deck;
2. A rectangle representing the landing deck;
3. A triangle representing the front wall of the deck, whose two vertices represent the bottom corners of the front wall, whereas the third vertex represents the midpoint of the front wall;
4. An elevator bar displaying the midpoint of the landing deck in the lateral axis and the required final altitude of the helicopter relative to the deck; and
5. A red horizontal line depicting the synthetic horizon.

During the initial development, one experimental test pilot of the German Armed Forces, Technical Center for Aircraft and Aeronautical Equipment evaluated early versions of the SLS display concept. This pilot (age 41y) has a flight experience of 2,400 hours (h) as Pilot in Command (PIC) for rotorcraft systems and multiple type ratings for NH90, BELL UH-1D, and EC135 (including VFR and IFR). He has practical experience in flying with Night Vision Goggles (NVG, 400h), using HMDs either in real flight (NH90, 300h), or various HMD types in simulation (30h). Besides holding a test pilot license (TP 1), he reported having encountered DVE conditions below 800 m while flying VFR over open water.

The pilot provided valuable feedback and suggested improvements to the SLS conceptual design. Specifically, the pilot recommended adding a space-stable symbology on the flight deck that displays the line-up line of the landing pad. Space-stable is defined as symbology aligned to the éarths surface. In previous studies, the space-stable symbology was used in onshore precision hover tasks in DVE conditions (see Ref. [34]). The line-up line is a part of the standard flight deck markings and is used to indicate the path to be followed by the helicopter's fore-and-aft axis during an approach to achieve the correct landing position [60]. Therefore, a line-up line was integrated into SLS according to the procedures defined in the aeronautical design standard (ADS-33 PRF, [13]) and the helicopter operations from ships other than aircraft carriers (HOSTAC, [60]). These improvements led to an enhanced SLS (ESLS) concept, which is depicted in Figure 7. The magenta line-up line, as shown in Figure 7, is visible through the HMD during final recovery (from MAP to final touch down) and, as a space-stable hover symbology.

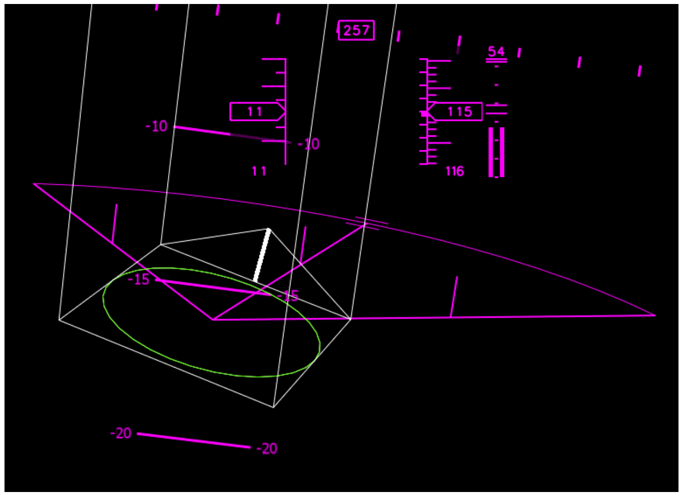

Figure 7. ESLS concept as seen through the HMD during shipboard approach

This symbology was stated as being familiar to all participating test pilots according to the standard course layout of the hover mission task element (MTE) [13]. However, for the simulated flights of this experiment, SLS concept was used for basic investigations of visual augmentation being activated and deactivated.

B. Control Augmentation Using Robust Sliding Mode Flight Controller

The notion of handling qualities (HQ) is often used to characterize the ease of piloting of helicopters [13] [21]. Using established quantitative and qualitative criteria, control designers and experimental pilots can predict and assign HQ levels on a scale from one to three, with level 1 indicating excellent handling. However, many bare-airframe, conventional helicopters tend to possesses poor handling quality ratings for the reasons discussed previously in Sec. II. The BO-105, whose flight dynamics model forms the basis of simulation in this research, is known to possess poor HQ for precision maneuvering tasks [61] [62]. Therefore, it becomes essential to augment the bare-airframe dynamics and simplify the helicopter's responses for the shipboard landing task.

Toward transforming the piloting task into a task of precisely steering the helicopter during the landing phase, this research explored four advanced helicopter response-types for the helicopter motion in the horizontal plane, namely the translational rate command with position hold (TRC/PH), and the acceleration command with velocity hold (ACVH). The response-types developed for the vertical and yawing motion are the well-known vertical rate command, height hold (RCHH), and yaw rate command, direction hold (RCDH), respectively. The flight envelope of interest was restricted to the hover and low-speed flight regime (up to 25 m/s forward speed). The synthesis of these different response-types is described next.

First, the TRC response-type maps the pilot's cyclic inceptor command as a linear function of the horizontal translational rate command. From the cyclic stick detent position in hover, a longitudinal cyclic command ($D_{\beta,c}$) yields a proportional change in the forward velocity ($V_{h,c}$), whereas a lateral cyclic command ($D_{\alpha,c}$) yields a proportional change in the lateral velocity ($V_{l,c}$).

$$\begin{aligned} V_{h,c} &= k_h \, \Delta D_{\beta,c} \\ V_{l,c} &= k_l \, \Delta D_{\alpha,c} \end{aligned}$$

where k_h and k_l are constant gains in the command model, and Δ denotes a change from the detent position. Returning the cyclic stick to the detent position commands zero translational rates ($V_{h,c} = 0, V_{l,c} = 0$), and the helicopter is expected to return to stable hover. Simplified helicopter translational equations of motion then yield the required pitch attitude change ($\Delta\theta = \theta_c - \theta_{trim}$) and the roll attitude change ($\Delta\phi = \phi_c - \phi_{trim}$) in order for the helicopter ground velocities (V_h, V_l) to track the commanded values.

$$\begin{aligned} \Delta\theta &\approx \left(V_h - V_{h,c}\right)/\mathrm{g} \\ \Delta\phi &\approx \left(V_l - V_{l,c}\right)/\mathrm{g} \end{aligned}$$

Second, the ACVH response-type maps the pilot's cyclic inceptor command as a linear function of the horizontal translational acceleration command. From the cyclic stick detent position, a longitudinal cyclic command ($D_{\beta,c}$) yields a proportional change in the forward acceleration ($\dot{V}_{h,c}$), whereas a lateral cyclic command ($D_{\alpha,c}$) yields a proportional change in the lateral acceleration ($\dot{V}_{l,c}$):

$$\dot{V}_{h,c} = k_h D_{\beta,c}$$
$$\dot{V}_{l,c} = k_l D_{\alpha,c}$$

where the constant gains k_h and k_l are not necessarily identical to the values of the gains in the TRC response-type. As before, returning the cyclic stick to the detent position should command zero acceleration, and the helicopter is expected to hold the ground velocity value at the time of return to detent. The required pitch and roll attitude commands in this case are:

$$\Delta\theta \approx \dot{V}_h/\text{g}$$
$$\Delta\phi \approx \dot{V}_l/\text{g}$$

Third, the RCHH response-type maps the pilot's collective inceptor command ($D_{\theta,c}$) as a linear function of the inertial vertical speed command ($V_{z,c}$) as follows:

$$V_{z,c} = k_z \Delta D_{\theta,c}$$

where k_z is a constant gain. An inertial to body transformation yields the commanded normal speed (w_c) as:

$$w_c = \frac{u \sin\theta - v \sin\phi \cos\theta + V_{z,c}}{\cos\theta \cos\phi}$$

Finally, the RCDH response-type maps the pilot's pedal command ($D_{\delta,c}$) as a linear function of the body yaw rate (r_c) as follows:

$$r_c = k_r \Delta D_{\delta,c}$$

where k_r is a constant gain. It is noted that the input command shaping constants (k_h, k_l, k_w, k_r) were determined to offer a balance between precision and aggressiveness; smaller gains allow finer, precise maneuvering but require considerable control deflections for aggressive maneuvers. Initial piloted simulation with the experimental test pilot of the German Armed Forces allowed fine-tuning of these gains.

The aforementioned input-command-shaping functions collectively yield a command vector $\boldsymbol{r} \equiv [\phi_c \quad \theta_c \quad w_c \quad r_c]^T$, which the helicopter output vector $\boldsymbol{y} \equiv [\phi \quad \theta \quad w \quad r]^T$ is required to track robustly (i.e., in the presence of any modeling uncertainties). For the subsequent attitude and rate control design, the nonlinear helicopter dynamics model described previously is linearized about equally-spaced airspeed intervals between hover and 25 m/s forward speed. The linearization process uses a built-in trim subroutine in the nonlinear model. Numerical perturbations about the trim states then yield the following linear state-space form:

$$\dot{\boldsymbol{x}} = \boldsymbol{Ax(t)} + \boldsymbol{Bu(t)}$$
$$\boldsymbol{y} = \boldsymbol{Cx(t)}$$

where $\boldsymbol{x} \equiv [\phi \quad \theta \quad u \quad v \quad w \quad p \quad q \quad r]^T$ and $\boldsymbol{u} \equiv [D_\theta \quad D_\alpha \quad D_\beta \quad D_\delta]^T$ are the state and control vectors, respectively, (u, v, w) represent the fuselage translational components in the body-frame, and (p, q, r) represent the fuselage angular rates in the body-frame. Further, $\boldsymbol{A}, \boldsymbol{B}$ are matrices containing the stability and control derivatives, respectively, and $\boldsymbol{C}$ is the output matrix. Stability analysis of this linear state-space model shows that the phugoid mode is unstable, the Dutch roll mode is stable but has low damping with a variable period, and the high frequency rotor lead-lag mode has very low damping [63]. These flight characteristics make the piloting of the BO-105 helicopter difficult. They also corroborate the findings of previous studies that highlight low HQ levels for precision maneuvering tasks [62].

The flight controller in this work employs the sliding mode control technique for generating the necessary actuator commands on the main and tail rotor blades for robust output tracking, such that $\lim_{t\to\infty} \|\boldsymbol{y} - \boldsymbol{r}\| = \boldsymbol{0}$. The subsequent steps in the sliding mode flight controller synthesis are identical to those described in Ref. [63], and are therefore omitted here for brevity. Reference [63] also discusses the level of agility, axial decoupling, and predicted HQ levels achievable by the sliding mode flight controller.

The pilot controller in ROSIE is a conventional center stick for cyclic control, a collective lever, and foot pedals. For the TRC response-type, the pilot commands on the cyclic inceptor are mapped onto the commanded translational rates in the local inertial reference frame. Thus, a longitudinal cyclic deflection yields a proportional forward velocity, and a lateral cyclic deflection yields a proportional lateral velocity. Cyclic detent holds the helicopter's current position.

For the ACVH response-type, the pilot commands on the cyclic inceptor are mapped onto the commanded translational accelerations in the local inertial reference frame. Thus, a longitudinal cyclic deflection yields a proportional forward acceleration, and a lateral cyclic yields a proportional lateral acceleration. Cyclic detent holds the helicopter's current velocities. The attitude command, attitude hold (ACAH) response-types for the pitch and roll attitudes are synthesized in the inner-loop for TRC and ACVH execution. Furthermore, the pilot's collective stick deflection yields a proportional inertial vertical speed. Collective detent holds altitude, and so this response is modeled as a rate command, height hold (RCHH) response-type.

Lastly, the pilot's pedal deflection yields a proportional yaw rate. Pedal detent holds heading, and so this response is modeled as a rate command, direction hold (RCDH) response-type. To satisfy ideal, lower-order responses using ADS-33 criteria, ACAH is modeled as a second-order transfer function, and RCDH and RCHH are modeled as first-order transfer functions.

V. Pilot-in-the-Loop Experiment

The purpose of the simulation testing was to assess pilot workload and handling qualities in the HSDI, with and without the support of visual and control augmentation techniques. The scope of the testing was to quantify workload and HQ for different sea states by simulating three levels of ship motion intensity. Four mission task elements were identified as contiguous elements of the shipboard recovery mission [60] [64]. The test participants included four experimental test pilots from the military and rotorcraft industry. Pilot workload was measured using the Bedford rating scale [43], task load index (NASA-TLX) weighting rating scale [56], and HQ levels were evaluated using the Cooper-Harper rating scale [65].

A. Ship Motion-Based Data

To explore the pilot's workload during the shipboard landing task, the used ship motion-based data as investigated in this chapter is connected to the specified MTEs as detailed in Chapter B. Therefore, the two types of motions of the ship, roll and heave, are isolated and detailed for the duration of the landing task to allow investigations on the effects of different motions. In order to structure the landing task during the experiment, all four MTEs are set to approximately a maximum 40 sec. of constant endurance and continuous transition between the MTEs. However, the pilots may fail in time or fulfillment of each MTE; each landing task run is continued through all 4 MTEs. Therefore, the implemented SCONE offers a long-lasting and almost constant setting for each chosen level of intensity of about 50 min. To account for the helicopter's attitude and acceleration disturbances, which are related to pilot workload, the roll and heave levels will be used during the simulator experiments to investigate an expected increase of the subjective workload and difficulty of fulfilling the recovery task. Furthermore, the roll attitude of the ship is balanced between the rolling to the left side and the right side from the perspective of the flying helicopter behind the deck. The heave levels of the ship between the heave up and heave down are balanced as well, again seen from the perspective of the flying helicopter behind the deck. A detailed view on the SCONE data roll and heave levels is given in Table 2.

Table 2. Comparison of the roll and heave levels within SCONE

Type of motion	Levels according to SCONE	Mean values	Maximum values
Roll left	1	1.95°	7.99°
Roll right	1	- 1.85°	- 7.35°
Roll left	2	4.06°	17.53°
Roll right	2	- 3.90°	- 18.09°
Roll left	3	5.31°	23.74°
Roll right	3	- 5.48°	- 26.92°
Heave up	1	0.98 ft/sec	5.35 ft/sec
Heave down	1	- 0.98 ft/sec	- 5.96 ft/sec
Heave up	2	1.95 ft/sec	11.71 ft/sec
Heave down	2	- 1.91 ft/sec	- 10.83 ft/sec
Heave up	3	3.64 ft/sec	19.18 ft/sec
Heave down	3	- 3.65 ft/sec	- 16.67 ft/sec

Even though the mean roll angles of the different levels range from Level 1 with 1.9° to Level 2 with 3.98° and up to Level 3 with 5.39° using all recorded roll angles of roll left and right, the maximum roll angles are much higher than its mean values and mean maxima values, as shown in **Table 2**. The mean maximum values in roll angles range from Level 1 with 2.92° (SD 1.64°) and -2.78° (SD 1.51°) to Level 2 with 5.85° (SD 3.59°) and -5.61° (SD 3.51°) and up to Level 3 with 7.21° (SD 5.15°) and -7.43° (SD 5.34°). These two aspects have to be taken into account, with both regarding the workload assessment when it comes to possible effects while using space-stable and non-space-stable visual augmented elements of the SLS and different advanced response types of the PAS during the landing task, and in detail during the MTE 1, MTE 2, MTE3, and MTE 4.

B. Shipboard Recovery Mission Task Elements

The simulation testing used the standard ship-controlled approach procedure reported in Refs. [60],[64] to isolate the landing sequence, as shown in Figure 8. The shipboard recovery mission [66] essentially combines the bob-up, bob-down maneuver and the sidestep maneuver from ADS-33E-PRF [65]. Thus, the mission sequence for testing purposes was defined using four contiguous MTEs from the missed approach point until touchdown on the landing deck. These include hover alongside the deck (MTE1), side step (MTE2), precision hover over deck (MTE3), and land on the deck (MTE4). The sequence of MTEs is shown graphically in Figure 8, and requires the pilot to execute the following tasks:

- Decelerate from translating flight to a stabilized hover alongside the ship deck with precision and a reasonable amount of aggressiveness (Figure 8, point (1)); thereafter, hold relative position, altitude, and heading alongside the ship deck (Figure 8, point (1));
- Sidestep to the center of the ship landing deck and attain stabilized hover (Figure 8, point (2));
- Hold relative position, altitude, and heading above the landing deck (Figure 8, point (3));
- Descend until touchdown during quiescent periods of the ship's roll and heave motion (Figure 8, point (4)).

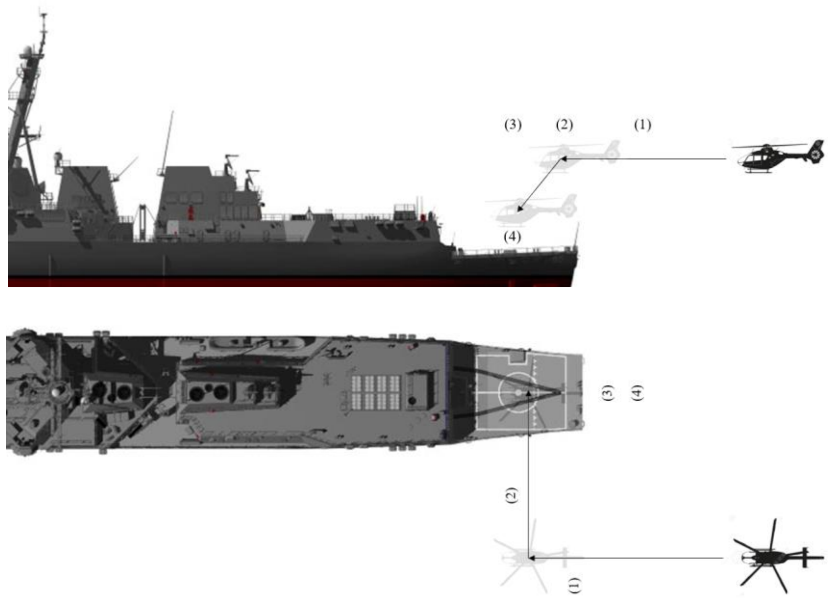

Figure 8. Side view (top) and top view (buttom) showing the shipboard recovery MTEs (figure not to scale)

C. Experimental Setup

Four experimental test pilots were invited on separate days to perform simulation tests. Of these, three are affiliated to the German Armed Forces, and the fourth pilot is affiliated to Airbus Helicopters. All pilots have extensive flight test experience, including in shipboard launch and recovery operations as pilot in command (PIC). Furthermore, all pilots have previously flown and evaluated both HMD systems and advanced control laws on both attack and utility helicopters (including the EC665 Tiger and the NH-90 NATO Frigate Helicopter). The pilots hold helicopter type ratings on AS350, AW139, AW189, Bell UH 1D, Bell-205, Bell 407, Bell 412, Bo-105, CH-53, EC-155, H-135, H-145, NH-90, Sea King, Sea Lion, Sea Lynx, Super Puma, and EC665-Tiger among them. Table 3 shows their anonymized experience data in flight testing and on helicopter simulators.

Table 3. Summary of the test pilot data[5]

Number of pilots	Age Mean (SD)	Helicopter experience as PIC Mean (SD)	Simulator experience as PIC Mean (SD)	Helicopter experience with HMD as PIC Mean (SD)	Simulator experience using HMD as PIC Mean (SD)
4	51.0 y (9.5 y)	4,353.8 h (1,493.4 h)	437.5 h (149.3 h)	712.5 h (661.3 h)	74.0 h (85.2 h)

The simulation exercises included an initial but a limited warm-up session for familiarization purposes. The warm-up sessions were also designed to allow a step by step familiarization of the helicopter dynamics model, the cockpit setup, the helicopter-ship interface, and the systems for visual and control augmentation.

Table 4: Independent variables for the simulation testing

SCONE Ship Motions	Visual Augmentation	Control Augmentation
Low intensity	Primary HDD	Primary FCS
High intensity	HMD + SLS	TRC/PH + RCDH + RCHH
		ACVH + RCDH + RCHH

Table 4 highlights the independent variables in terms of the ship motion levels and the visual and control augmentation levels for the design of the experiments. Note that only two levels of ship motion were chosen (Level 1 and Level 3), because the intention was to capture the effect of ship motion and not to characterize operational limits. The ship speeds in all cases was maintained between 20 kts and 23 kts with a constant course of 270°. Furthermore, the visibility conditions for the entire experiment was fixed to 800 m from the helicopter center, which corresponds to the instrument flight rules, category 1 minimum visibility.

All combinations of the independent variables led to twelve test cases that were then evaluated by each pilot. The overall duration of the simulation exercises was time-limited to avoid fatigue effects, discomfort, and the effects thereof on the workload metrics. Moreover, all pilots followed an identical sequence of MTEs as shown in Figure 8. All MTEs were flown under nominal system behavior and system degradations or failures were excluded.

D. Data Collection Methods

Data from two sources were collected during the piloted simulation tests. The first source was data recordings of the flight dynamics, flight control, and the ship motion, which forms the basis of the flight trajectory performance (discussed in the following section). These data were recorded with a frame rate of 100 Hz, and include such aircraft states and controls as positions, attitudes, velocities, accelerations, angular rates, cylic, collective, and pedal inputs, and the pilot's head motion while using the HMD system.

The second data source was human performance measured using workload metrics and the assigned handling qualities ratings. Pilot workload was measured using two well established rating techniques: the Bedford workload rating scale commonly used in experimental testing during highly demanding piloting tasks [67], and the deck interface pilot effort scale (DIPES) that is specifically tailored to be used with fleet pilots during deck landings [68].

The 10-point Bedford scale shown in Figure 9 quantifies pilot workload; a rating of 1 indicates low workload whereas 10 indicates that the task has to be abandoned. The Bedford scale is useful to determine the pilot's spare capacity to perform tasks in addition to the one being evaluated. For the present research, the Bedford scale was used to evaluate the impact of the proposed visual and control augmentation techniques on pilot workload generated by primary piloting task; the lower this workload, the more spare capacity the pilot would have to accept additional mission tasks. Moreover, pilot workload was detailed in its characteristics by using NASA-TLX [69] scale. NASA-TLX is a multi-dimensional scale designed to obtain workload estimates from one or more operators while they are performing a task or immediately afterwards.

[5] SD = standard deviation; PIC = pilot in command; y = years; h = hours

Also shown in Figure 9, DIPES requires pilots to rate a 5-point scale on the basis of their workload, performance, accuracy and consistency during landing. A DIPES rating of 3 or better indicates that safe and precise deck landings can be repeatedly achieved. Although DIPES has been widely used to predict ship helicopter operational limits, its use in the present research was primarily aimed at understanding the potential of visual and control augmentation techniques to improve safety during deck landings.

The helicopter handling qualities during the mission task elements were evaluated using the well known Cooper-Harper handling qualities rating (HQRs) scale [70]. Following its definition, it was of interest for the present research to determine the ease and precision of the pilot-vehicle system to achieve the desired performance with the proposed visual and control augmentation techniques. The level of handling qualities is determined from the HQR that pilots assign on a scale from 1 to 10; a level 1 handling makes the system desirable whereas a level 3 handling indicates major deficiencies.

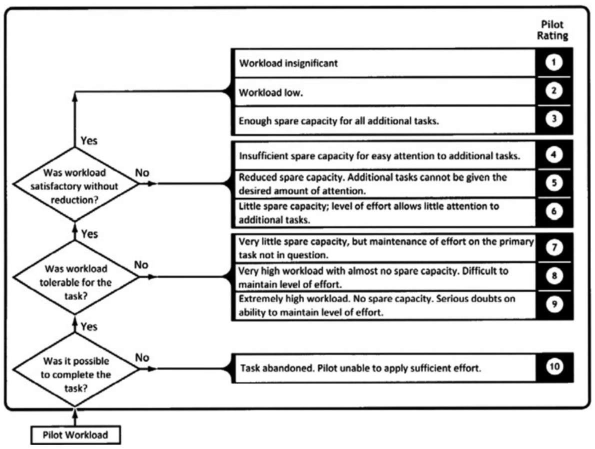

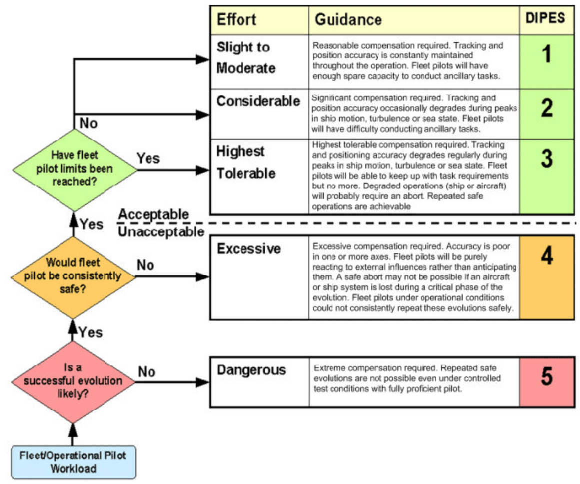

Figure 9: Bedford rating scale (left) and DIPES (right)

Aside from the workload and HQ questionnaires, each pilot also reported on the simulator sickness questionnaire upon completion of the simulation exercises. The questionnaire provided in Ref. [71] was used for this purpose. The responses indicated that none of the pilots faced motion sickness, except for slight fatigue, sweating and fullness of the head.

E. Elements of Observations

Beside a subjective analysis focusing on pilot workload and rating of SLS, handling qualities rating according to ADS-33 PRF [13], analysis of the flight path of helicopter-ship interface, and inspection of the pilot's behavior in detail control inputs and pilots view angles were investigated in regard to the pilot's performance [72].

The qualities or characteristics of an aircraft that govern the ease and precision with which a pilot can perform the tasks required to support the aircraft mission are known as handling qualities [73]. Handling qualities encompass all aspects of the human-machine interface: This includes cockpit ergonomics, the choice and design of the visual augmentation, the field of view, presentation and update rate of the display of the HMD, the available advanced flight response types and the vehicle's response to small, moderate, and large amplitude inputs. The metrics presented in the Cooper Harper Levels 1-3 provide a consistent boundary with Bedford Workload Levels 1-3. Furthermore, the DIPES rating and TLX weighted Cooper Harper rating delivers a contribution to detailed aspects of effort, frustration, mental workload, physical demand, temporal demand, and performance [73].

Important input and flight state parameters were recorded with a frame rate of 100 Hz, e.g., helicopter position, attitude, velocity, acceleration, angular rates, the primary control axis input, head motion while using HMD, together with display settings and visibility conditions. The HMD view was simultaneously rendered for the instructor, who was sitting behind the pilot to verify correct settings and viewing conditions.

The main goals of this study, taking in account subjective and objective analysis, are as follows:

1. To focus attention on and investigate the connections between subjective pilot rating and pilot-vehicle system performance [74].
2. To allow an assessment of visual augmentation, in detail the ESLS.
3. To evaluate the two advanced response types, TRC and ACVH.
4. And finally, to examine the PAS in total using visual and control augmentation.

VI. Results and Discussion

A. Assessment of Subjective Workload

Figure 10 shows that all four MTEs received Bedford ratings of predominantly level 2 up to level 1 with control augmentation, while the ratings without control augmentation were level 3, particularly during more intensive ship motion. Due to the way the Bedford scale is structured via the questions the pilot must answer, a change in rating from 4 to 3 is a significant improvement indicating that the workload is satisfactory without reduction and that the pilot still has spare capacity to accept additional tasks. A Bedford workload of level 1 was almost reached with a combination of control and visual augmentation, as shown in Figure 10. Furthermore, the ACVH response-type was found to induce lower workload as compared to the TRC response-type. This observation was also confirmed from pilot statements that a velocity hold feature was easier and more intuitive for landing on a moving deck.

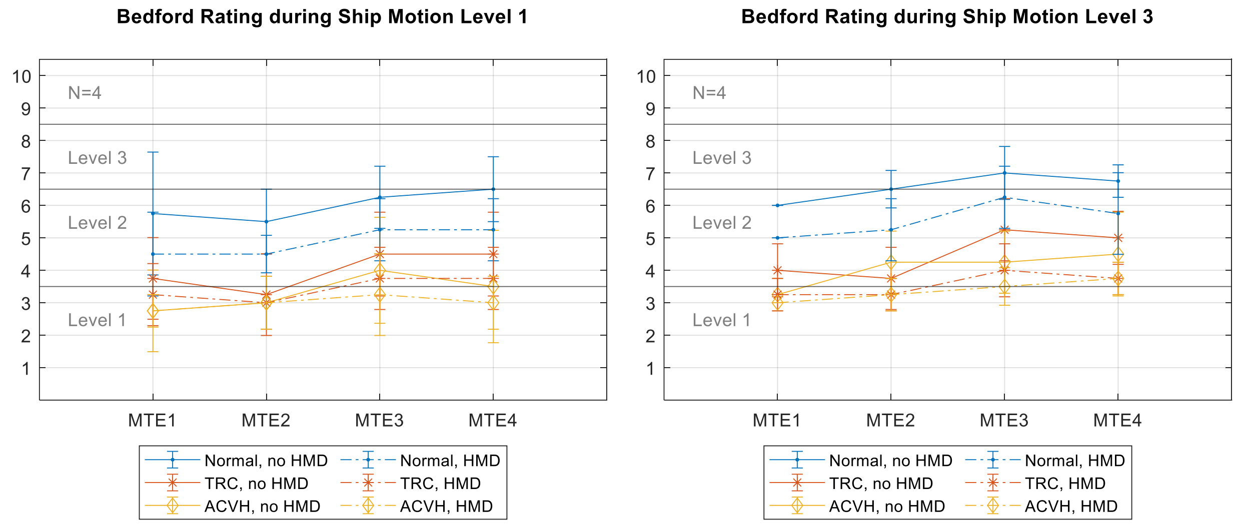

Figure 10. Pilot's workload rating (mean/SD) of MTEs during low and high ship motions (*4 PILOTS*)

With regards to the different MTEs, the mean workload ratings for MTE1 and MTE2 are comparable, and so are the mean ratings for MTE3 and MTE4. Furthermore, the mean workload during MTE3 and MTE4 is generally higher than the workload during MTE1 and MTE2. That was confirmed orally by the pilots: During MTE3 and MTE4 workload on keeping a safe distance from the rear wall of the deck (obstacle awareness) was coming on top to manuevering workload. Moreover, for all the cases with control augmentation, there is little further reduction in the workload rating with the HMD-SLS. This observation is in line with the pilots' comments; the helicopter was more stable with control augmentation and the pilots could perform all the MTEs with fewer control inputs. Moreover, most of the pilots reported that the HMD-SLS system allowed them to have the landing spot and deck front wall in sight at all times and they benefited from the see-through capabilities of the HMD.

Regarding the Bedford workload rating during low and high intensity ship motions as also shown in Figure 10, almost all MTEs received similar ratings. Furthermore, similar ratings for different motion levels of the ship were observed while the pilots benefitted from the PAS including control and visual augmentation in contrast to normal controls. These ratings fit the pilots' comments that ship motion becomes a factor from the point on where the helicopter enters the edge of the ship deck (from MTE2 to MTE3). Pilots reported that increased ship motion led to increased vertigo, which could be compensated by a visual fixation of a space-stable point of the ship. By flying with visual cues only (HMD plus normal controls), the pilots reported that they focused on the virtual point around which the ship rolls and not on the synthetic horizon while using the HMD-SLS.

Figure 11 and Figure 12 may confirm the above findings. Figure 11 and Figure 12 show the workload weighting related to frustration (F), mental demand (MD), physical demand (PD), temporal demand (TD), performance (P), and effort (E) during low and high ship motions. Overall, the TLX index increased on MD, TD; P, and E from low to high ship motions. This was confirmed orally by the pilots: The closer pilots flew to the deck, the more MD was needed. Moreover, high maneuvering compensations (TD, P, E) were needed when coming closer to the ship to be aware of the heaving landing deck and rear deck wall to not hit them with the landing gear and rotor tail. Generally, with a focus on MTE3 and MTE4, as also shown before in the Bedford workload rating, the TLX weighting increased during these two MTEs when the helicopter entered the edge of the deck.

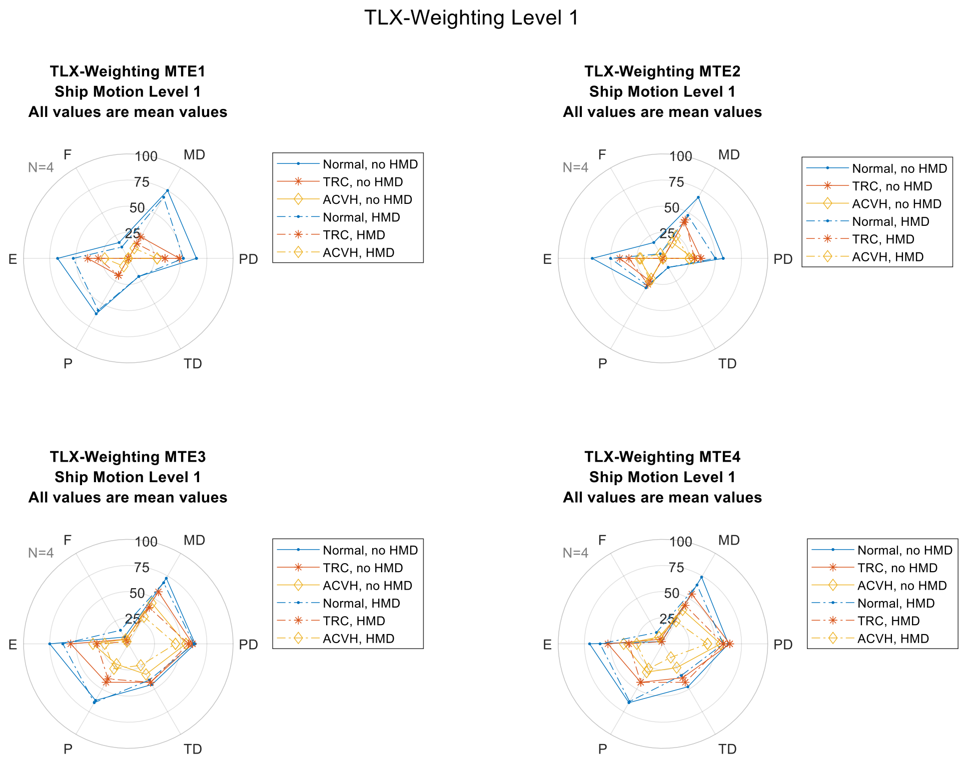

Figure 11. Pilots' TLX weighting (mean) of MTEs during low intensity ship motion (4 pilots)

Effort, mental demand, physical demand, and performance were rated higher than frustration and temporal demand over all four MTEs. Frustration may be not have been a factor because all pilots successfully completed all MTEs. Moreover, temporal demand was not observed because execution time was not performance factor, and unexpected events or system degradations were excluded from the simulation testing.

Regarding different control augmentations, pilots strongly benefited during MTE1 and MTE2. Pilots commented that fewer control inputs were needed to keep the helicopter stable during hover alongside and even during the sidestep maneuver. Besides that, the pilots commented that they were able to observe the ship's general behavior during both low intensity and high intensity ship motions due to the increased spare capacity. During MTE3 and MTE4, pilots reported that the TRC and ACVH modes improved (E, P) the situation to maneuver and keep the helicopter over the deck. Furthermore, the pilots reported both response-types to be sufficiently aggressive (P) to maneuver the helicopter as precisely as possible over the center of the landing pad. The ACVH response-type was even rated with a lower TLX weighting than the TRC response-type as shown in Figure 11, which again was consistent with the pilots' comments. They observed that the ACVH mode felt more "intuitive" than the TRC mode.

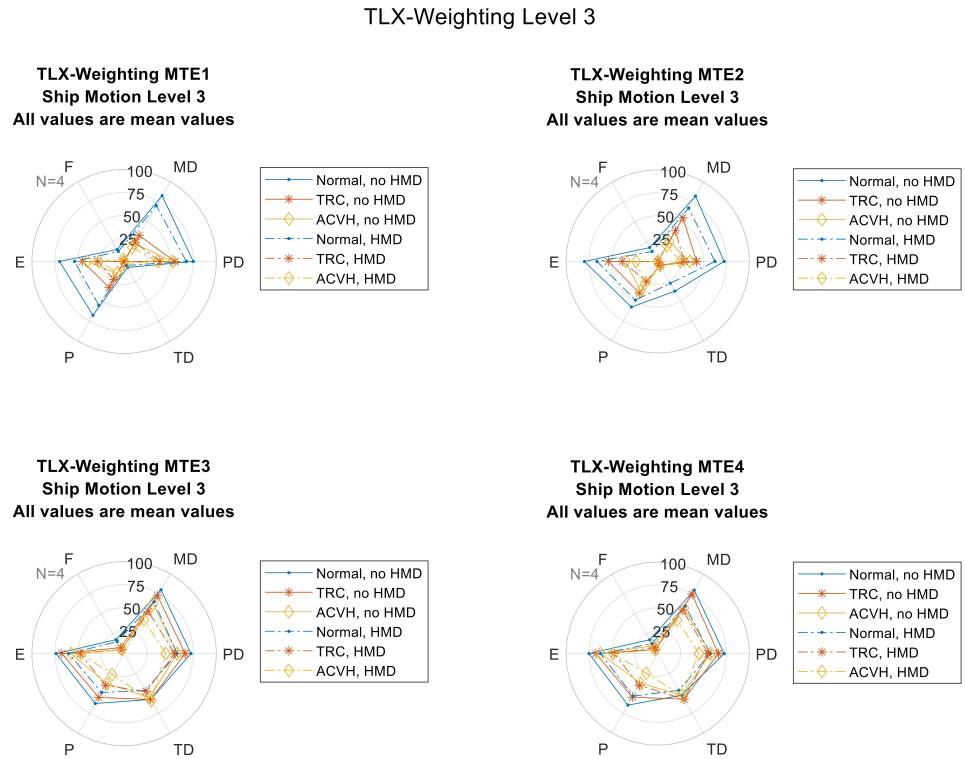

Figure 12. Pilots' TLX weighting (mean) of MTEs during high ship motions (4 pilots)

As the ship motion intensity increased, the pilots' rating of the temporal demand increased, especially during MTE3 and MTE4 as seen in Figure 12. This observation can be attributed to an increased time pressure in that pilots tried to avoid a hard landing on the deck in the presence of higher intensity ship heave motion.

Finally, Figure 13 depicts the pilots' DIPES ratings during low and high ship motions, with and without visual and control augmentation. An important consideration in DIPES is that ratings are assigned based on the perceived ability of an average fleet pilot. Although a highly capable test pilot may be able to safely land for a given ship motion, a rating may be awarded that excludes this condition from the envelope if it is deemed difficult for a fleet pilot to perform on a regular basis. As shown in Figure 10, a change in rating from 4 to 3, was a significant improvement to the point where the flown maneuver is acceptable or not for a fleet pilot.

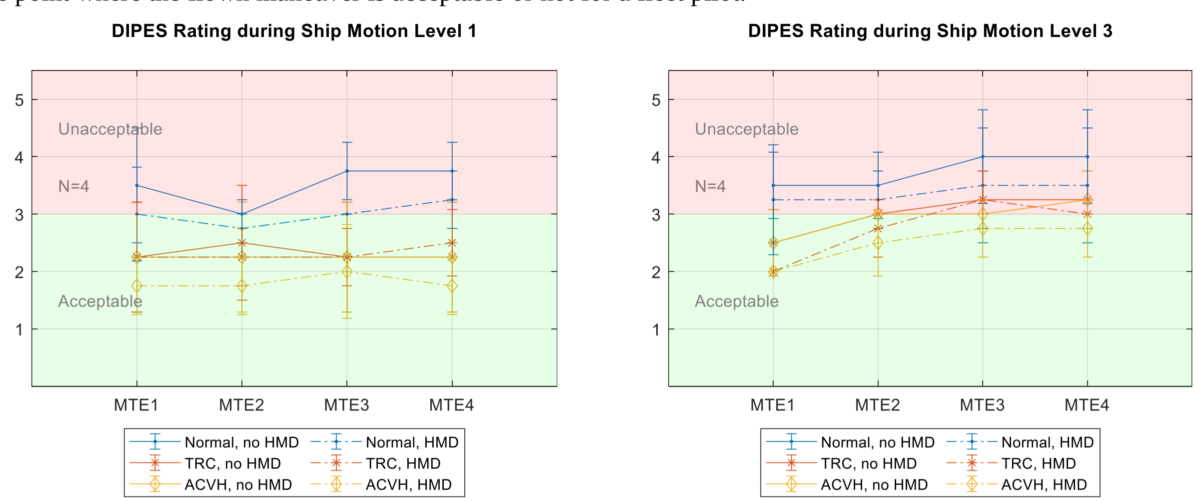

Figure 13. Pilots' DIPES rating (mean/SD) of MTEs during low and high ship motions

The findings from the DIPES rating shed light on the perceived ability of fleet pilots to benefit from visual and control augmentation. In high intensity ship motion, MTEs 2 to 4 were perceived by the participating pilots to be too demanding and unsafe for fleet pilots, regardless of the use of the proposed control and visual augmentation. Only the ACVH response-type together with the HMD-SLS was considered acceptable had a borderline rating, which, for all practical purposes, was stated by the pilots as insufficient for the high level of ship motion intensity. On the contrary, in low intensity ship motion, all MTEs were consistently perceived to have acceptable workload in low intensity ship motion with the use of the proposed control and visual augmentation; in this case the ACVH response-type with HMD again received the best rating.

Next, Figure 14 shows the pilot assigned HQRs for all the cases. As expected, the biggest improvement in HQR resulted from the use of control augmentation. Both the TRC and the ACVH response-types lie well in the Level 1-2 HQR range. The ACVH response-type scored a notch higher, scoring Level 1 in low intensity ship motion and borderline Level 1 in high intensity ship motion. The bare-airframe, unaugmented dynamic responses lie were borderline Level 2-3. Furthermore, the difference in HQR across the four different MTEs was negligible. Finally, it can also be observed visual augmentation improved, although only marginally, the pilot assigned. This observation was expected because all cases used the same visual conditions. Should the shipboard approach procedures be conducted in degraded visual environment where fewer visual cues are available than in an onshore environment, it is expected, as previous studies also indicate [56] [34], that visual augmentation would play a more prominent role in pilot assigned HQRs.

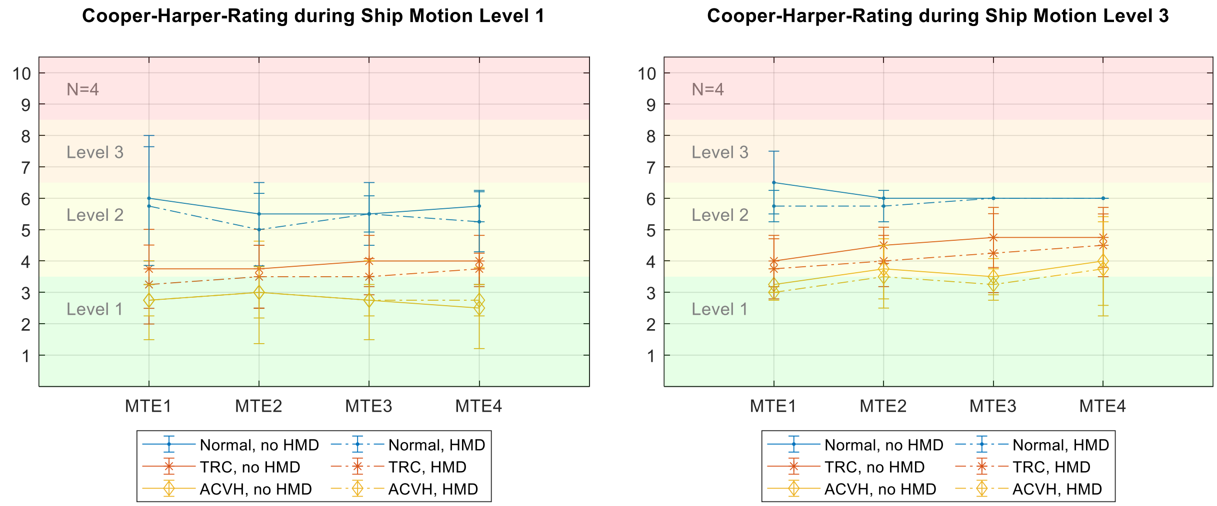

Figure 14. Pilots' HQR (mean/SD) of MTEs during low and high ship motions

B. Observations

Figure 15 and Figure 16 show traces of the helicopter position plotted on a y-z plane for low and high ship motion levels for a single pilot (PID4). These approach profiles are representative of the great majority of the landing trials performed with other pilots.

Figure 15 and Figure 16 show a more stable behavior of the helicopter at the start of the maneuver, which is most likely due to the helicopter being strongly subjected with the activated advanced response types mode ACVH in this off-deck location. Figure 15 and Figure 16 also illustrate a phenomenon that is observed in many of the approaches. During the hover alongside maneuvers, as the helicopter approaches the port-side deck edge, it declines several meters in height. This is due to the standard SBAS SOAP approach as the pilot tries to stabilize the helicopter at the height of the upper limit of the front wall of the moving deck. Moreover, the pilot navigates the helicopter beside the deck to harmonize with the ship's velocity. Figure 15 and Figure 16's left hand images show an effect that was observed during several hover alongside (MTE1) maneuvers: The helicopter entered pilot induced oscillations (PIOs), which were increasing with increasing ship motion levels from low to high. Pilot comments confirmed that this is realistic pilot control input behavior as the pilot focuses visually on the rolling and heaving flight deck. In contrast, with the PAS activated the pilots reported keeping the helicopter more stable. This phenomenon is commonly experienced in an approach to frigates using the ACVH mode, where minimal inputs are needed from the pilot to synchronize with the ship's velocity and front wall upper limit height. Moreover, the pilots reported to be able to have the landing spot in sight at all times (i.e., the spot being covered from the helicopter's shape and its cockpit instrumentation) by benefiting from the visual augmented augmentation.

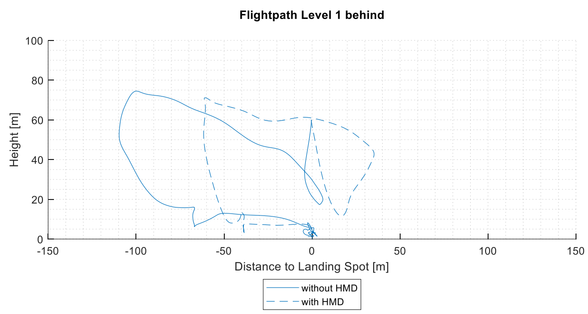

(a) Without control augmentation **(b) With control augmentation (ACVH)**

Figure 15. PID4 helicopter CG positions from behind the ship during low intensity ship motion

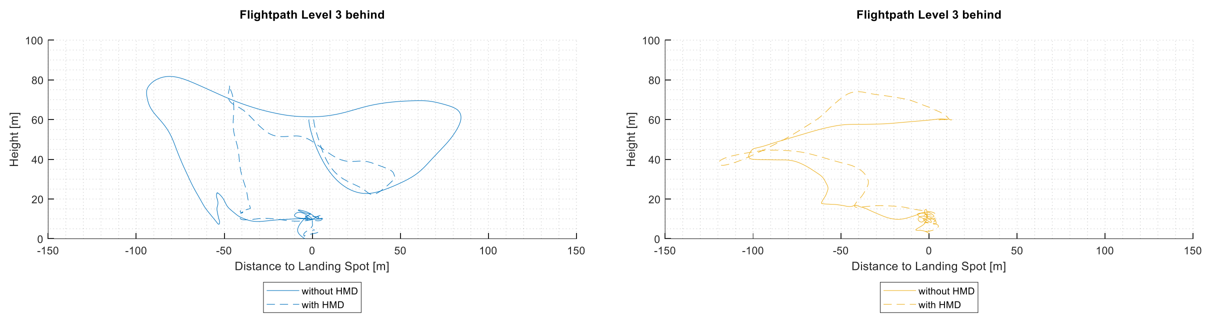

(a) Without control augmentation **(b) With control augmentation (ACVH)**

Figure 16. PID4 helicopter CG positions from behind the ship during high intensity ship motion

Figure 17 plots the side view of the flight paths of the pilots using the TRC and ACVH response-types modes in comparison to the primary flight controls, the following observations were made:

1. During mission task elements with both control augmentation activated, all pilots were able to execute more stable and precise flight paths (Figure 17).
2. Pilots commented that first, they synchronized the helicopter's forward speed with the speed of the ship (within a range of 20 to 23 kts ground speed) during MTE1. Then, they aligned with the ship's course (270°) during MTE1 and MTE2. By translating the helicopter directly over the deck during MTE3, pilots sought to use as few inputs as possible with cyclic control. However, during the final touchdown during MTE4, pilots stated that they acted on the lateral cyclic for a final alignment of the helicopter with the ship roll axis, and then pushed down collective during a quiescent period of the ship's movement for a stable touchdown.

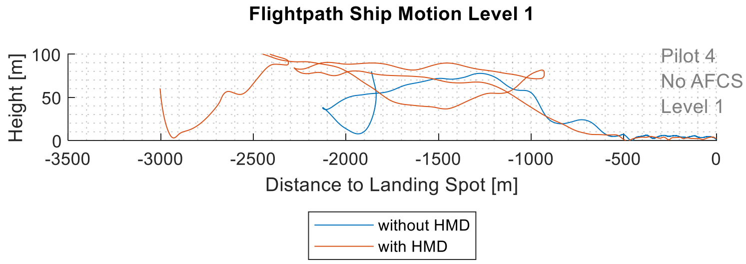

(a) Without control augmentation

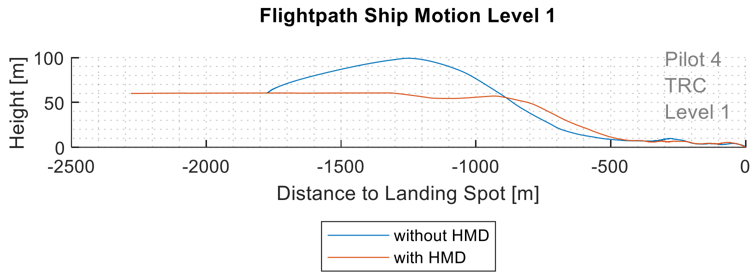

(b) With control augmentation (TRC)

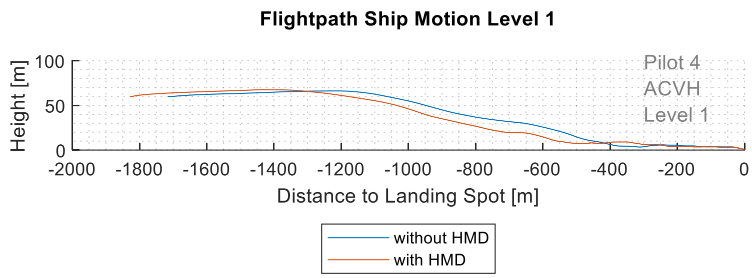

(c) With control augmentation (ACVH)

Figure 17. PID4 helicopter flight paths from the side during the deck approach

Figure 18 indicates lower pilot inputs in the cyclic channels with the activation of control augmentation. These plots corroborate pilot statements that control augmentation simplifies piloting and that the HMD-ESLS improved situational awareness. The main pilot comments were as follows:

1. Both TRC and ACVH allow an enhanced and more precise approach to the deck until landing. One test pilot from industry even commented that landing the helicopter on the deck with ACVH and HMD-ESLS is "a piece of cake". However, it is important to note that this pilot has more than 5,000 flight hours onshore and even more than 3,000 flight hours offshore.
2. All pilots commented that both TRC and ACVH response-types are sufficiently aggressive for the mission tasks. Even the latency from input of the pilot until feedback of the helicopter was rated to be good.
3. The TRC and ACVH response-types required successively lower pilot inputs. Three out of the four pilots commented that they found the ACVH response-type more more intuitive than the TRC response-type. However, it should be noted that all the participating pilots were trained to fly comparable control augmentation systems on the NH90 naval helicopter.

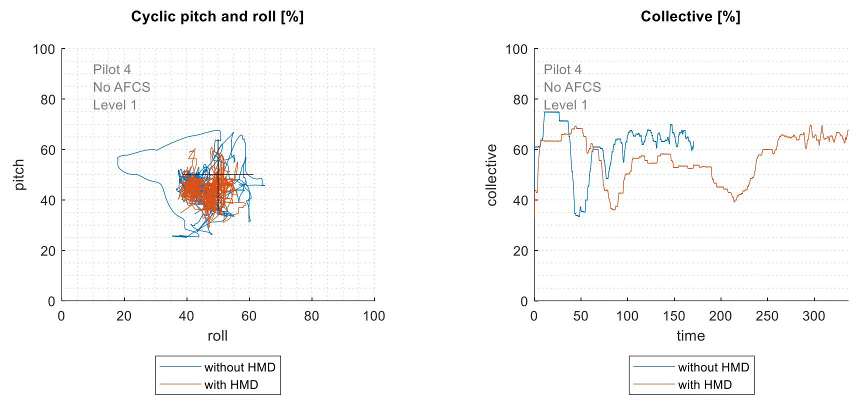

(a) Without control augmentation

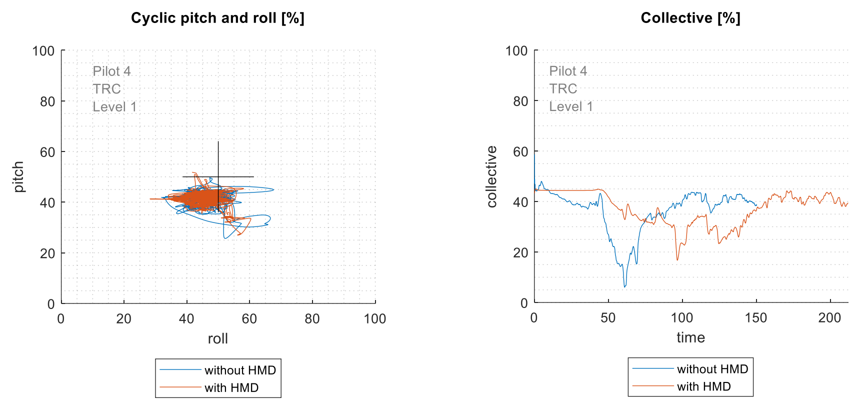

(b) With control augmentation (TRC)

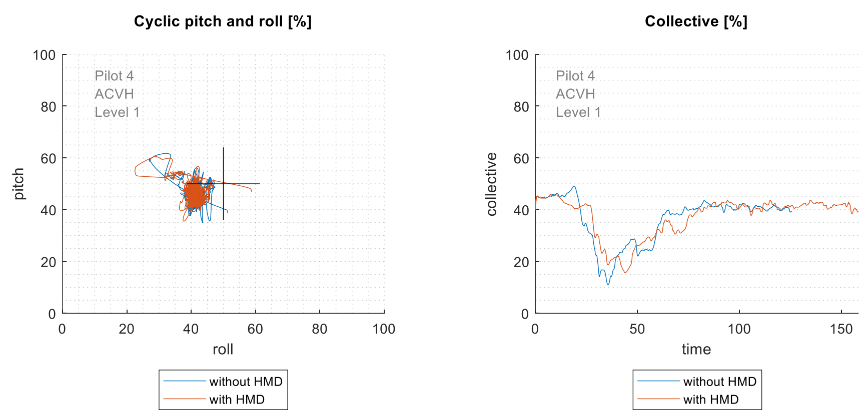

(c) With control augmentation (ACVH)

Figure 18. Cyclic and collective control activity during a deck approach with used PAS modes

In the final stages of approach during sidestep (MTE2) and hover over deck (MTE3), it was apparent that all pilots had a tendency to "drag the spot", to cross over the deck edge aft of the intended landing spot and to progress forward over the ship deck to the spot. Multiple pilots reported a self-observed tendency to drag the spot, and they suggested that this was a result of their efforts to maintain visual contact with the spot in the final stage of the maneuver. Most of the pilots reported keeping a safe distance in longitudinal position to the front wall of the deck by holding the cyclic control inputs in a backward position. The left tendency of the cyclic control inputs may arise from the goal to not overshoot the deck in lateral positioning during final recovery and initial trim configuration.

As discussed above, PIOs also turned out to be a factor during the final hover maneuvers over deck (MTE3) and land on the deck (MTE4). This could be a result from the fact that the moving front wall is now positioned directly in front of the helicopter, and therefore covers most of the pilot's field of regard. All pilots reported that they benefitted from the PAS at this stage of recovery: The advanced response types (TRC and ACVH) keep the helicopter in a stable position over the deck with minimal inputs needed from the pilot. Besides that, the pilots benefitted from the visually augmented ESLS; in detail, the elevator bar keeps the helicopter visually in the middle of the deck in the longitudinal axis and at a safe altitude referenced to the rolling and heaving landing spot at the same time. This effect may arise from the elevator bar acting as a virtual deck officer to enhance the pilot's control activity with unlimited visual reference in contrast to the deck officer, who is normally hidden by the cockpit instrumentation as discussed above.

Finally, the head movement of the pilot was recorded to obtain insights into pilot physical motion in the cockpit; this is plotted in Figure 19. The magnitude of head motion is found to decrease with increased levels of control augmentation. It may be stated that the main view of the pilot was in the lower horizontal section probably aiming the ship in front. That could arise mainly from the fact that pilots had to proceed with a descent to approach the deck. Three out of four pilots commented that the "see-through" capabilities of the HMD ESLS allowed them to perform an “eyes-out” approach to the ship with the deck in sight at all times. However, most of the pilots stated that they benefitted from the HMD ESLS mainly in combination with control augmentation.

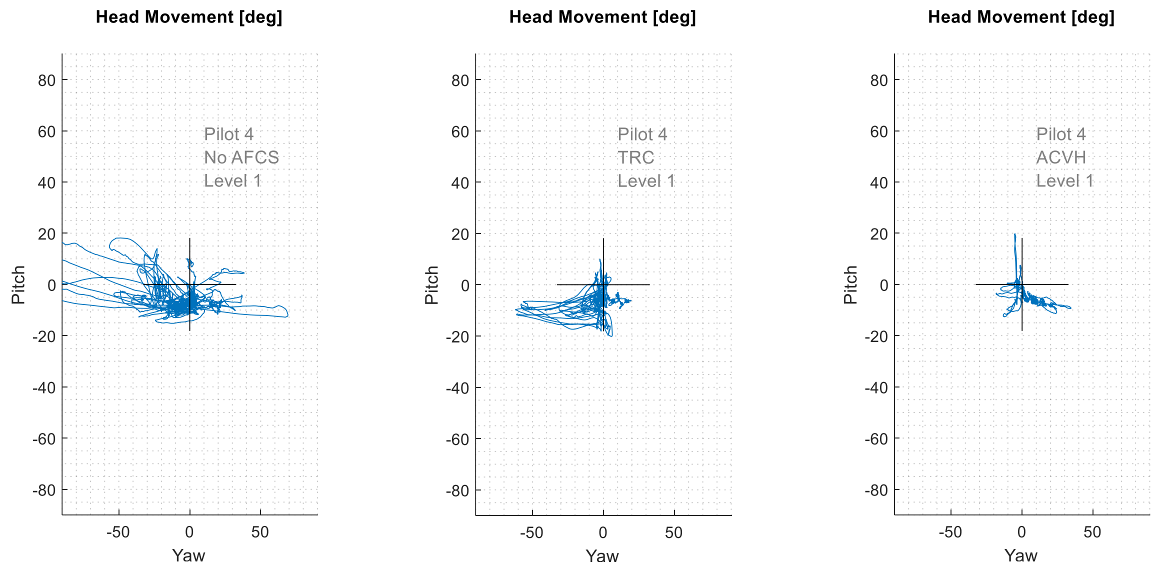

Figure 19. Head movement during a full deck approach task using HMD-SLS and advanced response-types

Major head movement effects of the HMD ESLS in combination to the advanced response types are discussed as follows:

1. All pilots commented that they had a generally emphasized view in the lower horizontal field of regard (FoR) while using HMD ESLS. It may be assumed that pilots tried to use the HMD ESLS to have the landing deck in sight at all times, and perform a straight-in approach while using TRC and ACVH in parallel.
2. The head movement of all pilots decreased with activated advanced response types. Again, all pilots commented that a combination of the HMD ESLS and the advanced response types allowed them to benefit from the HMD- displayed symbology and flight parameters while the helicopter needed fewer inputs due to enhanced controllability with the advanced response types.

C. Evaluation of Display Concept

All test pilots were invited to discuss and rate the ESLS concept used during the flights according to structured questionnaires and discussions after the experiment as shown in Figure 20. Therefore, questions about the elements of the ESLS as described earlier were rated by the pilots to identify benefits of the ESLS during different states of flight. In detail, each MTE included the same questions about

1. The two landing circles: Do you benefit from the landing circles in regard to the estimation of the altitude (1.1, 2.1, 3.1, 4.1) and position (1.2, 2.2, 3.2, 4.2) of the own helicopter relative to the landing deck.
2. The deck marking symbology: Do you benefit from the deck marking symbology projected on the HMD to have the deck in sight at all times (1.3, 2.3, 3.3, 4.3) and to keep the position (1.4, 2.4, 3.4, 4.4) of the own helicopter relative to the landing deck.
3. The synthetic horizon: Do you benefit from the synthetic horizon projected on the HMD to have the horizon in sight at all times (1.5, 2.5, 3.5, 4.5) and to keep the position (1.6, 2.6, 3.6, 4.6) of the own helicopter steady.

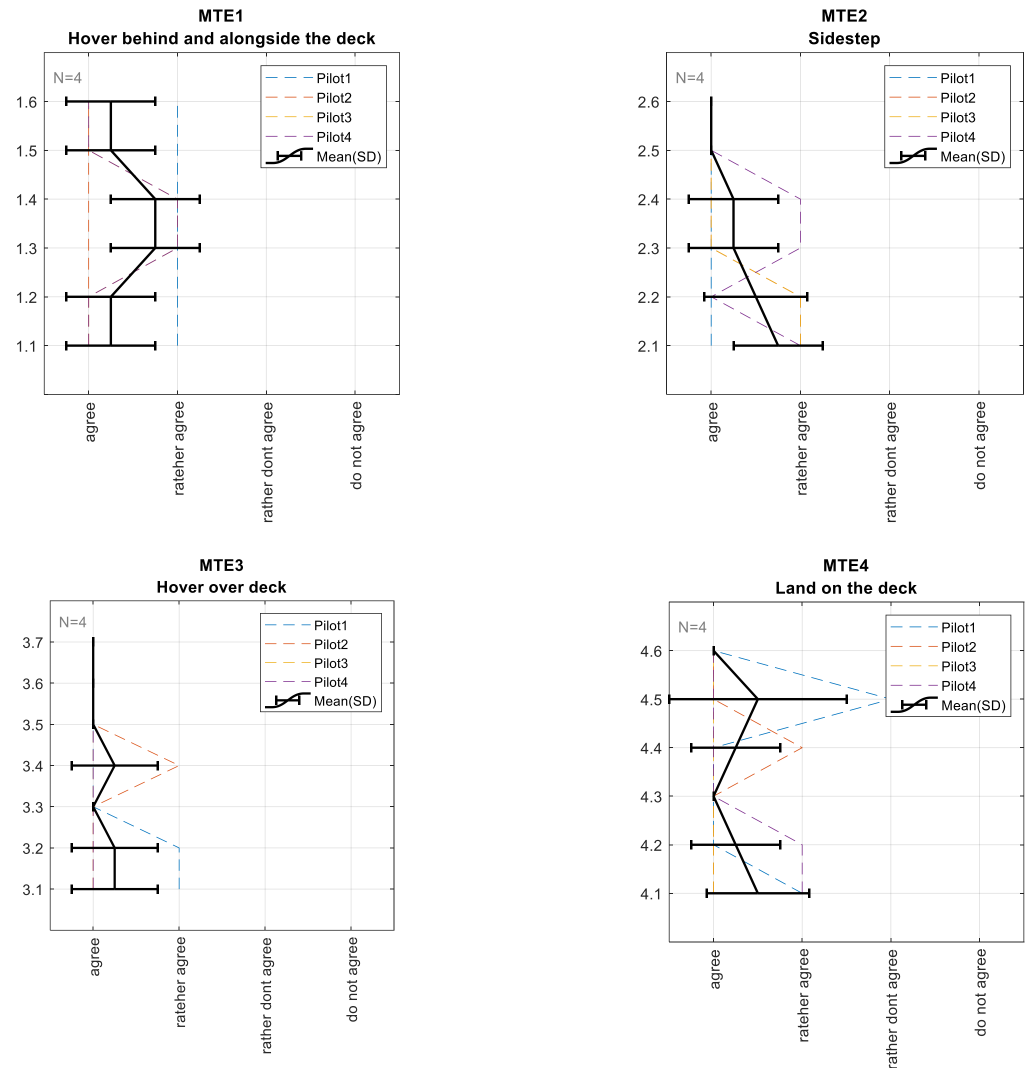

Figure 20. Test pilot's subjective rating of ESLS concept used in flight

All test pilots commented about the use of the landing circles in addition to the estimation of own position and altitude relative to the deck as well as finding the deck by the beginning of the maneuver. The ESLS projected on the HMD may improve the finding, approaching, and keeping of position relative to the deck with the limited visibility range (800 m, IFR CAT I) used during the experiments. However, with the visibility range of 800 m, the ship could also be detected visually in the sea. The test flights started in 60 ft AGL, 0.75NM behind the Missed Approach Point (MAP), so that the landing deck was barely visible.

Furthermore, two of four test pilots always recommended to have the deck in even better sight while hovering not directly besides, but a little further behind the deck (135° red wind direction). This position allowed all pilots to observe the movement of the ship and to anticipate the repeating rolling and heaving of the ship. Further, the maneuver keeping position over the landing deck, two out of four pilots commented looking "from time to time" through the cockpit instruments with the HMD to estimate their final landing position, ultimately before landing. However, most of the pilots agreed in further discussions that due to the higher workload during hover over deck and land, pilots concentrated more on the combination of the deck marking symbology and outside scenery.

The deck marking symbology, especially the front wall triangle and the elevator bar, was used by all pilots in order to enhance similar tasks: During hover alongside the deck, pilots used the 3D deck marking symbology to estimate the ship's behavior. The pilots benefited from the see-through capabilities of the HMD due to the covering effects of the ship by the cockpit instruments board and the A-pillar of the helicopter simulator. While proceeding with sidestep and hover over the deck, all pilots rated the triangle and the elevator bar to be very important. The triangle allowed the pilots to estimate their lateral position relative to the deck and, as they commented, "to find the ideal position in lateral axis to land". During this time, three out of four pilots agreed to use a combination of the triangle and the roomstable hover symbology to reach an ideal landing position in lateral and longitudinal axes.

With having the triangle and the elevator bar both in sight at the same time, the pilots further benefitted in regard to collision avoidance due to the elevator bar showing the altitude of the landing gear relative to the landing deck at all times. However, as mentioned above, during the final touchdown, all pilots agreed to focus on the elevator bar combined with the outside view of the moving ship.

This effect of concentrating on the elevator bar combined to the outside view during the "final push down" was confirmed by asking the pilots about the use of the synthetic horizon: three out four pilots recommended using the synthetic horizon mainly during hovering alongside the deck to keep the helicopter's position and to have a stable visual remark in the maritime environment. In regard to proceeding with the sidestep maneuver, the outside view (of the sea) became covered by the moving installations and the back wall of the moving ship. Subsequently, most of the pilots switched from focusing on the synthetic horizon to the deck landing symbology and the outside scenery, and in detail on the landing deck of the ship.

Finally, it may be supposed that a combination of the outside scenery and the see-through capabilities of the HMD and its projected 2D and 3D landing symbology fitted to the landing deck allowed the pilots to use both in harmonization. However, all pilots commented that the heads-up projected 2D flight parameters reduced a pilot's workload and enhanced the pilot's SA to have the main helicopters parameters, the outside scenery, and the assisting landing symbology in sight at all times.

VII. Conclusions

The ship-helicopter dynamic interface flight simulation of ROSIE has been described by its aspects of development, integration, and pilot-in-the-loop simulator flight tests of a newly developed Pilot Assistance System (PAS). The investigations were performed via fixed-base, pilot-in-the-loop flight simulation and included four professional (maritime) test pilots from the German Armed Forces and industry with extensive operational and test experience in shipboard environment. The maritime simulation environment is provided by the newly integrated DDG-51 type destroyer including the Systematic Characterization of the Naval Environment (SCONE) to the Rotorcraft Simulation Environment ROSIE, a simulation of the North Sea, and adjustable Degraded Vision Environments (DVEs) within a highly realistic weather model. Besides that, the maritime environment presentation of the simulated North Sea is enhanced by the integration of a 3D wave- and texture-model-based on the Gerstner waves theory tailored to the ship motion levels. The principle conclusions of the integrated maritime environment to ROSIE are summarized as follows: The specification of the ship deck landing task in the pilot-in-the-loop simulation contains the main MTEs according to the ADS-33 PRF [13] maritime standards. The ship-motion-based data as analyzed and integrated into ROSIE may allow a structured and reproducible use for pilot-in-the-loop simulator experiments. However, in this experiment, main ship motions (SCONE data sets "low" and "high") were used to investigate pilots' shipboard landing strategies according to standard naval procedures of SBAS SOAP and HOSTAC [60] [64].

The newly developed PAS included an HMD projected visual augmented Ship Deck Landing Symbology (SLS) tailored with two advanced response types, TRC - Translation Rate Command, and ACVH - Attitude Hold Velocity Command. Besides that, the 2D and 3D decluttered SLS symbology concept was discussed and improved to an enhanced SLS (ESLS) in two workshops in collaboration with two professional maritime test pilots from the German Armed Forces, who both have extensive experience in flying helicopters equipped with visually augmented IR sensors by an HMD. Equally, the advanced response types, TRC and ACVH, were tested and enhanced regarding aggressiveness and optimizing feedback latency together with a test pilot of the German Armed Forces holding multiple licenses on modern test and fleet helicopters.

Results from the current simulator study together with four maritime test pilots from the German Armed Forces and industry echo previous work demonstrating that flight in a harsh maritime environment is a great challenge, increasing pilot workload, increasing the necessity for pilot performance and reducing situational awareness. The current study, however, also indicated that these challenges could be greatly reduced if pilots had access to advanced response types and an HMD visual augmentation:

1. With access to advanced response types, pilot's level of workload decreased from Level 3 (no advanced response types), up to Level 1 using TRC or ACVH. Accordingly, handling qualities of all pilots decreased from Level 3 (no flight control assistance), up to almost Level 1 while using both advanced response types separately from each other. Comparing subjective workload assessments confirmed these results and indicated a preference for higher degrees of aircraft stabilization in the shipboard environment.
2. While increasing ship motions from the SCONE dataset, "low" and "high" pilot's workload increased and handling qualities rating decreased simultaneously, however workload kept almost within an acceptable level.

The used HMD ship deck landing symbology (SLS) further reduced a pilot's workload, and decreased TLX weighting based on the main aspects as follows: The intuitive HMD SLS visual augmentation concept was accepted well by all test pilots. However, all test pilots recommended that HMD SLS could further enhance the situation when operating the helicopter in DVEs, as done within the next experiment. The results of this study may demonstrate that access to a pilot assistance system, including pilot-fitted advanced response types and an HMD visual augmentation, would reduce the difficulties associated with flying in the maritime environment.

Acknowledgements

The work reported in this paper is funded by the Institute of Helicopter Technology at the TUM Technical University of Munich. The authors would like to thank all test pilots from the German Federal Armed Forces (WTD61, Technical Center for Aircraft and Aeronautical Equipment) in Manching, Germany and Airbus Helicopters (Flight Test Department) in Donauwörth, Germany for participating pro bono in the simulation testing and providing valuable feedback. The authors would also like to thank the U.S. Office of Naval Research for providing the SCONE dataset for used in this work. Finally, the authors wish to acknowledge the contributions to the simulation software development of the following students: Mr. Tibor Gasparac (University of Zagreb) and Mr. Maximilian Werhahn (Technical University of Munich).

References

[1] Lumsden, R. B., Padfield, G. d., and Braby-Deighton, C. D., “Human Factors Challenges at the Helicopter-Ship Dynamic Interface,” SAE Technical Paper Series, SAE International400 Commonwealth Drive, Warrendale, PA, United States, 1999. https://doi.org/10.4271/1999-01-5607

[2] “Modelling Helicopter Flight Dynamics: Building a Simulation Model,” Helicopter flight dynamics, edited by G. D. Padfield, 2nd ed., American Institute of Aeronautics and Astronautics; Blackwell Publishing, Washington DC, Oxford, 2008, pp. 87–185. https://doi.org/10.1002/9781119401087.ch3

[3] Lehmann, P. H., Jones, M., and Höfinger, M., “Impact of turbulence and degraded visual environment on pilot workload,” CEAS Aeronautical Journal; Vol. 8, No. 3, 2017, pp. 413–428. doi: 10.1007/s13272-017-0246-3.

[4] Wang, Y., White, M., Owen, I., Hodge, S., and Barakos, G., “Effects of visual and motion cues in flight simulation of ship-borne helicopter operations,” CEAS Aeronautical Journal; Vol. 4, No. 4, 2013, pp. 385–396. doi: 10.1007/s13272-013-0085-9.

[5] Yeh, M., Wickens, C. D., and Seagull, F. J., “Effects of Frame of Reference and Viewing Condition on Attentional Issues with Helmet Mounted Displays,” ARL-98-1/ARMY-FEDLAB-98-1, U.S. Army Research Laboratory, 1998.

[6] Mitchell, D. G., and Hoh, R. H., “Development of Time Response Criteria for Rotorcraft at Hover and Low Speed,” 12th Atmospheric Flight Mechanics Conference, AIAA Paper 1985-1790, Aug. 1985. Doi: https://doi.org/10.2514/6.1985-1790

[7] Hodge, S. J., Forrest, J. S., Padfield, G. D., and Owen, I., “Simulating the environment at the helicopter-ship dynamic interface: research, development and application,” The Aeronautical Journal; Vol. 116, No. 1185, 2012, pp. 1155–1184. doi: 10.1017/S0001924000007545.

[8] Wilkinson, C.H., Roscoe, M.F., and Vandervliet, G.M. Determining Fidelity Standards for the Shipboard Launch and Recovery Task, AIAA Paper No. 2001-4062, AIAA Modeling and Simulation Technologies Conference, Montreal, Canada, August 2001. doi: 10.2514/6.2001-4062.

[9] Viertler, F., Hajek, M., “Requirements and Design Challenges in Rotorcraft Flight Simulations for Research Applications,” AIAA SciTech - Modeling and Simulation Technologies Conference, Kissimmee, Florida, USA, 2015. https://doi.org/10.2514/6.2015-1808

[10] Lee, D., and Horn, J. F., “Simulation of Pilot Workload for a Helicopter Operating in a Turbulent Ship Airwake,” Proceedings of the Institution of Mechanical Engineers, Part G: Journal of Aerospace Engineering; Vol. 219, No. 5, 2005, pp. 445–458. doi: 10.1243/095441005X30298.

[11] Schwartz, A., "Systematic Characterization of the Naval Environment - Deck Motion Characterization," American Society of Naval Engineers Launch and Recovery Symposium, ASNE Publications, Alexandria, Virginia, USA, 2016.

[12] Viertler, F.; Hajek, M. (2015): Dynamic registration of an optical see-through HMD into a wide field-of-view rotorcraft flight simulation environment. In: Daniel D. Desjardins, Kalluri R. Sarma, Peter L. Marasco und Paul R. Havig (Hg.): Display Technologies and Applications for Defense, Security, and Avionics IX; and Head- and Helmet-Mounted Displays XX. SPIE Defense + Security. Baltimore, Maryland, United States, Monday 20 April 2015: SPIE (SPIE Proceedings), 94700Y. doi: 10.1117/12.2176190

[13] Aeronautical Design Standard, Handling Qualities Requirements for Military Rotorcraft, ADS-33D, U.S. Army Aviation and Troop Command, St. Louis, MO, July 1994.

[14] Wickens, C. D., Goh, J., Helleberg, J., Horrey, W. J., & Talleur, D. A. (2003). Attentional models of multitask pilot performance using advanced display technology. Human Factors, 45(3), 360–380. https://doi.org/10.1518/hfes.45.3.360.27250.
[15] Ernst, J. M., Doehler, H.-U., & Schmerwitz, S. (2016). A concept for a virtual flight deck shown on an HMD. In J. Sanders-Reed & J. J. Arthur (Eds.), SPIE Proceedings, Degraded Visual Environments: Enhanced, Synthetic, and External Vision Solutions 2016 (p. 983909). SPIE. https://doi.org/10.1117/12.2224933
[16] Wartmann, J., Zimmermann, M., Lüken, T., (2015) Abschlussbericht LuFo IV-Projekt HELIcopter Situation Awareness für eXtreme Missionsanforderungen (HELI-X). DLR-Interner Bericht, Projektbericht. DLR-IB 111-2015/12, 81 S. http://www.gbv.de/dms/tib-ub-hannover/828630119.pdf
[17] Padfield, G., Charlton, M., Kimberley, A., (1992). Helicopter Flying Qualities in Critical MTEs; initial experience with the DRA (Bedford) Large Motion Simulator. Retrieved from https://dspace-erf.nlr.nl/xmlui/bitstream/handle/20.500.11881/2452/ERF%201992-Vol2-F2.pdf?sequence=1&isAllowed=y
[18] Hodge, S. J., Forrest, J. S., Padfield, G. D., and Owen, I., "Simulating the environment at the helicopter-ship dynamic interface: research, development and application," The Aeronautical Journal; Vol. 116, No. 1185, 2012, pp. 1155–1184. doi: 10.1017/S0001924000007545.
[19] Owen, I., White, M. D., Padfield, G. D., and Hodge, S. J., "A virtual engineering approach to the ship-helicopter dynamic interface – a decade of modelling and simulation research at the University of Liverpool," *The Aeronautical Journal*; Vol. 121, No. 1246, 2017, pp. 1833–1857. doi: 10.1017/aer.2017.102.
[20] Forrest, J. S., Owen, I., Padfield, G. D., & Hodge, S. J. (2012). Ship-Helicopter Operating Limits Prediction Using Piloted Flight Simulation and Time-Accurate Airwakes. Journal of Aircraft, 49(4), 1020–1031. https://doi.org/10.2514/1.C031525
[21] Padfield, G.D., Controlling the Tension Between Performance and Safety in Helicopter Operations. A Perspective on Flying Qualities, Proceedings of the 24th European Rotorcraft Forum, Marseilles, France, September 1998. Retrieved from https://www.researchgate.net/publication/289544183_Rotorcraft_Handling_Qualities_Engineering_Managing_the_Tension_between_Safety_and_Performance_32nd_Alexander_A_Nikolsky_Honorary_Lecture, 17.04.2020.
[22] Moon, J., Domercant, J. C., & Mavris, D. (2015). A simplified approach to assessment of mission success for helicopter landing on a ship. International Journal of Control, Automation and Systems, 13(3), 680–688. https://doi.org/10.1007/s12555-013-0092-y.
[23] Carico, G. D., Fang, R., Finch, R. S., & Geyer Jr., W. P. (2003). Helicopter/ship qualification testing: Les essais de qualification hélicoptère/navire ([Elektronische Ressource]). AC/323(SCI)TP: Vol. 53. Neuilly-sur-Seine: NATO. Retrieved from http://www.rta.nato.int/Pubs/RDP.asp?RDP=RTO-AG-300-V22
[24] Soneson, G. L., Horn, J. F., and Zheng, A., "Simulation Testing of Advanced Response Types for Ship-Based Rotorcraft," Journal of the American Helicopter Society; Vol. 61, No. 3, 2016, pp. 1–13. doi: 10.4050/JAHS.61.032011.
[25] Radford, R. C., and Andrisani, D., "An experimental investigation of VTOL flying qualities requirements in shipboard landings," Journal of Aircraft; Vol. 21, No. 6, 1984, pp. 371–379. doi: 10.2514/3.44975.
[26] Lehmann, P. H., Jones, M., and Höfinger, M., "Impact of turbulence and degraded visual environment on pilot workload," CEAS Aeronautical Journal; Vol. 8, No. 3, 2017, pp. 413–428. doi: 10.1007/s13272-017-0246-3.
[27] Wang, Y., White, M., Owen, I., Hodge, S., and Barakos, G., "Effects of visual and motion cues in flight simulation of ship-borne helicopter operations," CEAS Aeronautical Journal; Vol. 4, No. 4, 2013, pp. 385–396. doi: 10.1007/s13272-013-0085-9.
[28] Cheung, B., McKinley, R. A., Steels, B., Sceviour, R., Cosman, V., and Holst, P., "Simulator Study of Helmet-Mounted Symbology System Concepts in Degraded Visual Environments," Aerospace medicine and human performance; Vol. 86, No. 7, 2015, pp. 588–598. doi: 10.3357/AMHP.4232.2015.
[29] Münsterer, T., Völschow, P., Singer, B., Strobel, M., & Kramper, P. (2015). DVE flight test results of a sensor enhanced 3D conformal pilot support system. In J. Sanders-Reed & J. J. Arthur (Eds.), SPIE Proceedings, Degraded Visual Environments: Enhanced, Synthetic, and External Vision Solutions 2015 (p. 947106). SPIE. https://doi.org/10.1117/12.2180634
[30] Zimmermann, M., Gestwa, M., König, C., Wolfram, J., Klasen, S., & Lederle, A. (2019). First results of LiDAR-aided helicopter approaches during NATO DVE-mitigation trials. CEAS Aeronautical Journal, 10(3), 859–874. https://doi.org/10.1007/s13272-018-0354-8
[31] Hensoldt (2020). SFERION Pilot Assistance during the entire mission under all conditions. Retrieved from https://www.hensoldt.net/fileadmin/hensoldt/Solutions/Air/Situational_Awareness/0361_17_Sferion_brochure_E_intranet.pdf, 29.03.2020.
[32] Tritschler, J. K., O'Connor, J. C., Pritchard, J. A., & Wallace, R. (2020). Exploratory Investigation into Rotorcraft Pilot Strategy and Visual Cueing Effects in the Shipboard Environment. Journal of the American Helicopter Society, 65(2), 1-13. https://doi.org/10.4050/JAHS.65.022003

[33] Watson, N. A., Owen, I., & White, M. D. (2020). Piloted Flight Simulation of Helicopter Recovery to the Queen Elizabeth Class Aircraft Carrier. Journal of Aircraft, 57(4), 742-760. https://doi.org/10.2514/1.C035733
[34] Viertler, F. X. (2017). Visual Augmentation for Rotorcraft Pilots in Degraded Visual Environment (Doctoral dissertation, Technische Universität München).
[35] Braun, D., Kampa, K., and Schimke, D., "Mission Oriented Investigation of Handling Qualities Through Simulation," 17th European Rotorcraft Forum, Deutsche Gesellschaft für Luft- und Raumfahrt, Bonn, Germany, 1991. doi: 10.1109/CGNCC.2014.7007598
[36] Dietz, M., Maucher, C., and Schimke, D., "Addressing Today's Aeromechanic Questions by Industrial Answers," American Helicopter Society Specialists' Conference on Aeromechanics, The Vertical Flight Society, Fairfax, VA, 2010.
[37] Johnson, W., "A History of Rotorcraft Comprehensive Analyses," American Helicopter Society 69th Annual Forum, The Vertical Flight Society, Fairfax, VA, 2013
[38] Viertler, F., and Hajek, M., "Evaluation of Visual Augmentation Methods for Rotorcraft Pilots in Degraded Visual Environments," Journal of the American Helicopter Society, vol. 62, no. 1, 2017, pp. 1–11.
[39] Doehler, H.-U., Ernst, J. M., and Lueken, T., "Virtual aircraft-fixed cockpit instruments," Proc. of SPIE Vol. 9471, Degraded Visual Environments: Enhanced, Synthetic, and External Vision Solutions, Baltimore, USA, 2015. https://doi.org/10.1117/12.2177796
[40] Aerial stern on view of the US Navy (USN) Arleigh Burke Class, June 2005. https://catalog.archives.gov/id/6669129. Date accessed: 17.09.2020.
[41] Viertler, F. and Hajek, M., "Requirements and Design Challenges in Rotorcraft Flight Simulations for Research Applications," AIAA Modeling and SimulationTechnologies Conference, AIAA Paper 2015-1808, Jan. 2015. doi: 10.2514/6.2015-1808
[42] Horn, J. F., Yang, J., He, C., Lee, D., & Tritschler, J. K. (2015). Autonomous ship approach and landing using dynamic inversion control with deck motion prediction. In 41st European Rotorcraft Forum 2015, ERF 2015 (pp. 864-877). (41st European Rotorcraft Forum 2015, ERF 2015; Vol. 2). Deutsche Gesellschaft fuer Luft und Raumfahrt (DGLR). ISBN (Electronic)9781510819832
[43] Minotra, D., and Feigh, K., "Studying Pilot Cognition in Ship-Based Helicopter Landing Maneuvers," AHS International 74th Annual Forum & Technology Display, Phoenix, Arizona, USA, May 14 – May 17, 2018.
[44] Horn, J. F., Yang, J., He, C., Lee, D., & Tritschler, J. K. (2015). Autonomous ship approach and landing using dynamic inversion control with deck motion prediction. In 41st European Rotorcraft Forum 2015, ERF 2015 (pp. 864-877). (41st European Rotorcraft Forum 2015, ERF 2015; Vol. 2). Deutsche Gesellschaft fuer Luft und Raumfahrt (DGLR).
[45] Zhao, D., Krishnamurthi, J., Gandhi, F., and Mishra, S., "Differential flatness based trajectory generation for time-optimal helicopter shipboard landing," 2018 Annual American Control Conference (ACC), IEEE, Piscataway, NJ, 2018, pp. 2243–2250. doi: 10.23919/ACC.2018.8430942
[46] Greer, W.B. and Sultan, C., "Shrinking Horizon Model Predictive Control Method for Helicopter–Ship Touchdown," Journal of Guidance, Control, and Dynamics, vol. 43, no. 5, 2020, pp.884-900. doi: 10.2514/1.G004374
[47] Mastin, G., Watterberg, P., and Mareda, J., 1987. Fourier Synthesis of Ocean Scenes. IEEE Comput. Graph. Appl. 7, 3 (March 1987), 16–23. doi: 10.1109/MCG.1987.276961
[48] World Meteorological Organization, "Guide to Wave Analysis and Forecasting: WMO-No. 702," https://www.wmo.int/pages/prog/amp/mmop/documents/WMO%20No%20702/WMO702.pdf, [retrieved 18 September 2020].
[49] Tate, S.J., "A Dynamic Challenge: Helicopter/Ship Interface Simulation – Development, Integration and Application," AGARD-CP-577, AGARD Flight Vehicle Integration Panel Symposium on 'Flight Simulation Where are the Challenges?', Braunschweig, Germany, May 1995.
[50] Tessendorf, J., "Interactive Water Surfaces," Game Programming Gems 4 , ed. Andrew Kirmse, Charles River Media, (2004).
[51] Tessendorf, J., (2001). Simulating Ocean Water. SIG-GRAPH'99 Course Note.
[52] Dupuy, J., Bruneton. E., "Real-time animation and rendering of ocean whitecaps," SIGGRAPH Asia 2012 Technical Briefs (SA '12). Association for Computing Machinery, New York, NY, USA, Article 15, 1–3. doi:10.1145/2407746.2407761
[53] Horvat, B., Hajek, M., and Rauleder, J., "Analysing Rotorcraft Vortex Encounter Methods with a Lattice-Boltzmann Method Based GPU Framework," AIAA Scitech Forum, AIAA Paper 2020-0539, Orlando, Florida, January 2020. doi: 10.2514/6.2020-0539
[54] Hodge, S. J., Forrest, J. S., Padfield, G. D., and Owen, I., "Simulating the environment at the helicopter-ship dynamic interface: research, development and application," The Aeronautical Journal; Vol. 116, No. 1185, 2012, pp. 1155–1184. doi: 10.1017/S0001924000007545.

[55] Lusardi, J. A., Tischler, M. B., Blanken, C. L., and Labows, S. J., “Empirically Derived Helicopter Response Model and Control System Requirements for Flight in Turbulence,” Journal of the American Helicopter Society, Vol. 49, No. 3, 2004, pp. 340–349. doi: 10.4050/JAHS.49.340
[56] Minotra, D., and Feigh, K., “Studying Pilot Cognition in Ship-Based Helicopter Landing Maneuvers,” AHS International 74th Annual Forum & Technology Display, Phoenix, Arizona, USA, May 14 – May 17, 2018.
[57] LCD29HMD Technical Characteristics, Trivisio Prototyping GmbH, URL: https://est-kl.com/images/PDF/Trivisio/LCD29-HMD_specifications.pdf , accessed: 26 August 2020.
[58] Jenkins, M. P., Hogan, C., and Kilgore, R., “Ecological display symbology to support pilot situational awareness during shipboard operations,” 2015 IEEE International Inter-Disciplinary Conference on Cognitive Methods in Situation Awareness and Decision Support (CogSIMA), IEEE, Piscataway, NJ, 2015, pp.213–219. doi: 10.1109/COGSIMA.2015.7108200
[59] Stanton, N. A., Plant, K. L., Roberts, A. P., Allison, C. K., and Harvey, C., “The virtual landing pad: facilitating rotary-wing landing operations in degraded visual environments,” Cognition, Technology & Work, Vol. 20, (2), 2018, pp. 219–232. https://doi.org/10.1007/s10111-018-0467-1
[60] “MPP-02(H)(1), Vol I, Helicopter Operations from Ships other than Aircraft Carriers (HOSTAC),” [online], https://www.japcc.org/wp-content/uploads/MPP-02-VOL-I-EDH-V1-E.pdf, [retrieved 17 June 2019].
[61] Ockier, C. J., “Flight Evaluation of the New Handling Qualities Criteria Using the BO105,” Journal of the American Helicopter Society, Vol.41, No. 1, 1996, pp. 67–76. doi: 10.4050/JAHS.41.67
[62] Ockier, C. J., and Gollnick, V., “ADS-33 Flight Testing—Lessons Learned,” AGARD Conference Proceedings 592: Advances in Rotorcraft Technology, Canada Communication Group, Hull (Quebec), Canada, 1996, pp. 10.1–10.12.
[63] Halbe, O, and Hajek, M.., “Robust Helicopter Sliding Mode Control for Enhanced Handling and Trajectory Following,” Journal of Guidance, Control, and Dynamics, 2020, article in advance. doi: 10.2514/1.G005183
[64] UK CAA, and Flight Ops 2, “CAA PAPER 2010/01 - The SBAS Offshore Approach Procedure (SOAP),” [online], https://publicapps.caa.co.uk/docs/33/2010001.pdf, [retrieved 17 June 2019].
[65] Carignan, S. J. R. P., Gubbels, A. W., and Ellis, K., “Assessment of Handling Qualities for the Shipborne Recovery Task-ADS 33 (Maritime),” American Helicopter Society 56th Annual Forum Proceedings, Virginia Beach, VA, May 2–4, 2000.
[66] Wang, Y., White, M., Owen, I., Hodge, S., and Barakos, G., “Effects of visual and motion cues in flight simulation of ship-borne helicopter operations,” CEAS Aeronautical Journal; Vol. 4, No. 4, 2013, pp. 385–396. doi: 10.1007/s13272-013-0085-9.
[67] Roscoe H., Ellis A & A., G. (1990), “A Subjective Rating Scale for Assessing Pilot Workload in Flight: A decade of Practical Use”, RAE report TR90019, Royal Aircraft Establishment, Farnborough, UK.
[68] Carico, G.D., Fang, R., Finch, R.S., Geyer, W.P., Krijns H.W., and Long, K., “Helicopter/Ship Qualification Testing,” Flight Test Techniques Series – Volume 22, North Atlantic Treaty Organisation, Neuilly-Sur-Seine Cedex, France, 2003.
[69] Hart, S. G., “Nasa-Task Load Index (NASA-TLX); 20 Years Later,” 2016; Proceedings of the Human Factors and Ergonomics Society Annual Meeting, 50(9), 904-908. doi: 10.1177/154193120605000909.
[70] Cooper, G.E., and Harper, Jr., R.P., The Use of Pilot Rating in the Evaluation of Aircraft Handling Qualities, NASA TN D-5153, Apr. 1969.
[71] Kennedy, R. S., Lane, N. E., Berbaum, K. S., and Lilienthal, M. G., “Simulator Sickness Questionnaire: An Enhanced Method for Quantifying Simulator Sickness,” The International Journal of Aviation Psychology; Vol. 3, No. 3, 1993, pp. 203–220. doi: 10.1207/s15327108ijap0303_3.
[72] Mitchell, D., Nicoll, T., Fallon, M., and Roark, S., “Rotorcraft Handling Qualities for Shipboard Operations,” AIAA Atmospheric Flight Mechanics Conference, [American Institute of Aeronautics and Astronautics], [Reston, VA], 2009. https://doi.org/10.2514/6.2009-6057
[73] Matayoshi, N., Forrest, J. S., Hodge, S. J., Padfield, G. D., & Owen, I. (2009). “Relationship between pilot workload and turbulence intensity for helicopter operations in harsh environments.” In Annual Forum Proceedings - AHS International Vol. 2 (pp. 1595-1603).
[74] Vrdoljak, M., Halbe, O., Mehling, T., and Hajek, M., “Simulator Experiments for Modeling Helicopter Pilot in Roll Tracking Task,” AIAA Science and Technology Forum 2020, Orlando, USA, January 2020. https://doi.org/10.2514/6.2020-2269